INTERNATIONAL JOURNAL FOR NUMERICAL AND ANALYTICAL METHODS IN GEOMECHANICS
*Int. J. Numer. Anal. Meth. Geomech.*, 2002; **26**:1449–1476 (DOI: 10.1002/nag.253)

# Elastic solutions for stresses in a transversely isotropic half-space subjected to three-dimensional buried parabolic rectangular loads

Cheng-Der Wang[1,*,†] and Jyh-Jong Liao[2]

[1]*Department of Civil Engineering, Nanya Institute of Technology, Chung-Li 320, Taiwan, R.O.C.*
[2]*Department of Civil Engineering, National Chiao-Tung University, Hsin-Chu 300, Taiwan, R.O.C.*

SUMMARY

In many areas of engineering practice, applied loads are not uniformly distributed but often concentrated towards the centre of a foundation. Thus, loads are more realistically depicted as distributed as linearly varying or as parabola of revolution. Solutions for stresses in a transversely isotropic half-space caused by concave and convex parabolic loads that act on a rectangle have not been derived. This work proposes analytical solutions for stresses in a transversely isotropic half-space, induced by three-dimensional, buried, linearly varying/uniform/parabolic rectangular loads. Load types include an upwardly and a downwardly linearly varying load, a uniform load, a concave and a convex parabolic load, all distributed over a rectangular area. These solutions are obtained by integrating the point load solutions in a Cartesian co-ordinate system for a transversely isotropic half-space. The buried depth, the dimensions of the loaded area, the type and degree of material anisotropy and the loading type for transversely isotropic half-spaces influence the proposed solutions. An illustrative example is presented to elucidate the effect of the dimensions of the loaded area, the type and degree of rock anisotropy, and the type of loading on the vertical stress in the isotropic/transversely isotropic rocks subjected to a linearly varying/uniform/parabolic rectangular load. Copyright © 2002 John Wiley & Sons, Ltd.

KEY WORDS: analytical solutions; stresses; transversely isotropic half-space; three dimensional; buried; linearly varying, uniform, and parabolic rectangular loads

## 1. INTRODUCTION

Anisotropic deformability is common in foliated metamorphic, stratified sedimentary and regularly jointed rock masses. Existing closed-form solutions, assuming linear and isotropic elasticity, for stress in such rocks or rock masses are normally not realistic. Better results can only be obtained by considering anisotropic deformability. Practically, an anisotropic rock can be modelled as either an orthotropic or a transversely isotropic material. This work derives

*Correspondence to: Cheng-Der Wang, Department of Civil Engineering, Nanya Institute of Technology, 414, Chung-Shan E. Road. Sec.3, Chung-Li 320 Taoyuan, Taiwan, R.O.C.
†E-mail: cdwang@nanya.edu.tw

Contract/grant sponsor: National Science Council of the Republic of China; contract/grant number: NSC 91-2211-E-253-002



*Received 27 August 2001*
*Revised 19 June 2002*

elastic solutions for stresses in a transversely isotropic half-space subjected to three-dimensional, buried, linearly varying/uniform/parabolic rectangular loads.

Numerical methods, graphical methods, and closed-form solutions can be used to calculate the stresses induced by external loads in an anisotropic half-space. The numerical procedures can easily be automated with modern computers. However, most contributions have addressed the calculation of stresses/displacements in isotropic media. The authors have proposed graphical method of computing stress/displacement in transversely isotropic rocks subjected to three-dimensional, irregularly shaped surface loads [1,2]. The use of anisotropic influence charts to calculate the stresses/displacements is fast. However, the advantages of using the influence charts decline if the loading region is not uniform or stresses/displacements at multiple depths are simultaneously sought. Therefore, the closed-form solution method to estimate the stresses induced by non-uniform loads may be an alternative to the numerical or graphical method.

A point load solution forms the basis of solutions to complex loading problems. Several researchers have presented solutions for stresses or displacements in response to a concentrated force applied to transversely isotropic half-spaces [3–5]. Wang and Liao [1,6] detailed various anisotropic loading conditions to obtain solutions in cases other than those that involved point loads. Stresses in a transversely isotropic half-space subjected to an arbitrary shape loaded area can be estimated by dividing the loaded area into several regularly shaped sub-areas, including triangles or rectangles. The authors recently derived closed-form solutions for stresses and displacements in a transversely isotropic half-space subjected to uniform/linearly varying triangular loads [7]. However, only uniform and some linearly varying rectangular loads acting on the transversely isotropic half-space were presented [6,8]. In many engineering fields [9,10], applied loads are not uniformly distributed but more concentrated towards the centre of the foundation. Hence, loads may be more realistically simulated as being distributed as linearly varying or as parabola of revolution. Teferra and Schultze [11] obtained solutions for stresses beneath the centre of a load in an isotropic half-space, for vertical concave and convex parabolic loads of infinite length. Nevertheless, existing closed-form solutions for anisotropic half-spaces are available only for axisymmetric problems. Gazetas [12,13] analytically investigated how soil's transverse isotropy affects stress distributions when it is subjected to axisymmetric parabolic vertical surface loading. To our knowledge, no closed-form solution for stresses in a transversely isotropic medium subjected to three-dimensional, buried, parabolic asymmetric loads has been proposed. Integrating the point load solutions in a Cartesian co-ordinate system [6] yields analytical solutions for stresses in the half-space caused by linearly varying/parabolic rectangular loads. The derived solutions are clear and concise. Also, according to our results, the buried depth, the dimensions of the loaded region, the type and degree of material anisotropy, and the loading type all affect stresses in a transversely isotropic half-space. An illustrative example is presented at the end of this paper to elucidate the effect of the dimensions of the loaded area, the type and degree of rock anisotropy, and the type of loading on vertical stress in isotropic/transversely isotropic rocks subjected to a linearly varying/uniform/parabolic rectangular load.

## 2. SOLUTIONS FOR STRESSES INDUCED BY LINEARLY VARYING AND PARABOLIC RECTANGULAR LOADS

In this work, the solutions for stresses in a transversely isotropic half-space subjected to three-dimensional, buried, linearly varying, uniform and parabolic rectangular loads are directly

 

integrated from the point load solutions in a Cartesian co-ordinate system [6]. Planes of transverse isotropy are assumed to be parallel to the horizontal surface. Appendix A provides closed-form solutions for stresses subjected to a point load $(P_x, P_y, P_z)$ that acts at $z = h$ (measured from the surface) in the interior of a transversely isotropic half-space.

In the case of point load solutions, $p_{s1i} \sim p_{s8i}$ is defined in Equations (A1)–(A6) as the elementary functions for stresses. The solutions for stresses in a transversely isotropic half-space subjected to linearly varying and parabolic rectangular loads can be directly obtained by integrating the elementary functions of the point load solutions. The closed-form solutions for stresses induced by linearly varied loads distributed over a rectangular area are first given below.

### 2.1. Linearly varying rectangular loads

A three-dimensional, upwardly linearly varying load, $P_j^{\text{linear}}$ $(j = x, y, z)$ (forces per unit area) distributed on a rectangle of length $L$ and width $W$ at a buried depth of $h$ as shown in Figure 1 is

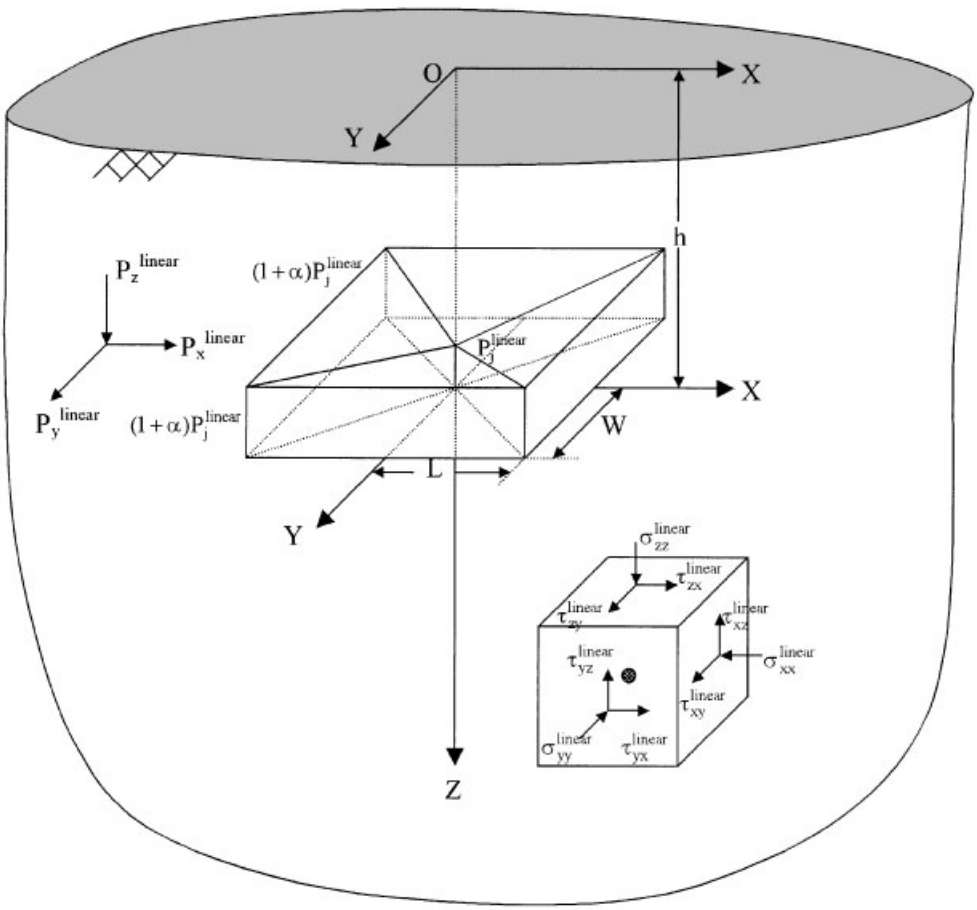


Figure 1. The case of upwardly linearly varying rectangular loads with $L*W$ area at the buried depth of $h(\alpha > 0)$.

 

considered. The loading type in Figure 1 can be expressed as the following form

$$\tilde{P}_j^{\text{linear}} = P_j^{\text{linear}}\left[1 + \alpha\left(\frac{|x|}{L} + \frac{|y|}{W} - \frac{|xy|}{LW}\right)\right] \tag{1}$$

where $\alpha$ is a constant. According to Equation (1), $\alpha$ specifies three different loading cases.

*Case* 1: $\alpha > 0$, the load is upwardly linearly varying as depicted in Figure 1;

*Case* 2: $\alpha = 0$, the load is uniform, as shown in Figure 2(a);

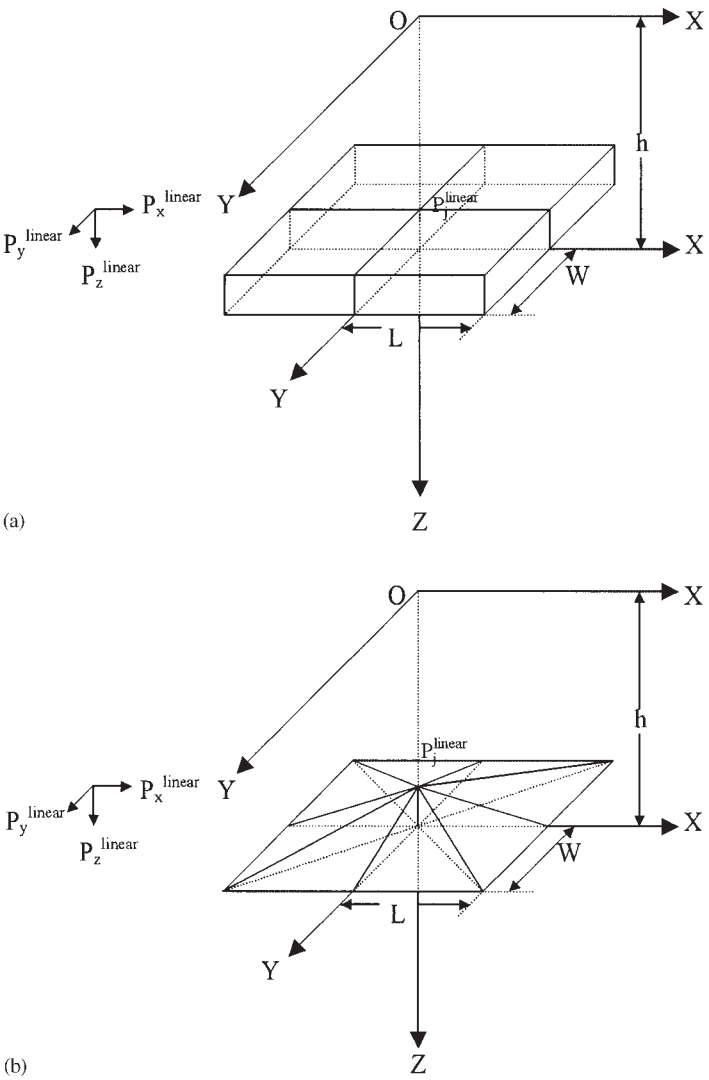


Figure 2. (a) The case of uniform rectangular loads with $L*W$ area at the buried depth of $h(\alpha = 0)$; (b) the case of a completely downwardly linearly varying rectangular loads with $L*W$ area at the buried depth of $h(\alpha = -1)$.

 

*Case* 3: $\alpha<0$, the load is downwardly linearly varying. Figure 2(b) shows zero contact stress applied to the region at the edges of Figure 1 in the case $\alpha=-1$.

An elementary force $\tilde{\boldsymbol{P}}_j^{\text{linear}}\,\mathrm{d}\eta\,\mathrm{d}\varsigma$, acting on an elementary surface $\mathrm{d}\eta\,\mathrm{d}\zeta$, is extracted from the rectangle to calculate the stresses in the transversely isotropic half-spaces. Replacing the concentrated force $P_j$ by $\tilde{\boldsymbol{P}}_j^{\text{linear}}\,\mathrm{d}\zeta\,\mathrm{d}\eta$, $y$ by $(y-\eta)$, and $x$ by $(x-\zeta)$ in Equations (A1)–(A6) yields solutions for stresses under the action of the elementary force in the half-space. Integrating the solutions with respect to $\eta$ from 0 to $W$, and with respect to $\zeta$ from 0 to $L$, we can derive the complete solutions:

$$[\sigma]^{\text{linear}}=\int_0^L\int_0^W[\sigma]^p\,\mathrm{d}\eta\,\mathrm{d}\varsigma \tag{2}$$

where $[\sigma]=[\sigma_{xx},\sigma_{yy},\sigma_{zz},\tau_{xy},\tau_{yz},\tau_{xz}]^{\mathrm{T}}$ (superscript, T, denotes the transpose matrix) and the superscripts, linear and $p$, refer to the stress components induced by a linearly varying rectangular load and a point load, respectively. The explicit solutions for stresses in a half-space can be regrouped in the forms of Equations (A1)–(A6). The exact solutions in this case are therefore just Equations (A1)–(A6), except that the stress elementary functions $p_{s1i}$, $p_{s2i},\ldots,$ $p_{s8i}$ are replaced by the stress integral functions $N_{s1i}^{\langle1\rangle}$–$N_{s1i}^{\langle4\rangle}$, $N_{s2i}^{\langle1\rangle}$–$N_{s2i}^{\langle4\rangle},\ldots,N_{s8i}^{\langle1\rangle}$–$N_{s8i}^{\langle4\rangle}$ ($i=1,2,3,a,b,c,d,e$) for $\sigma_{xx}^{\text{linear}}$, $\sigma_{yy}^{\text{linear}}$, $\sigma_{zz}^{\text{linear}}$, $\tau_{xy}^{\text{linear}}$, $\tau_{yz}^{\text{linear}}$, $\tau_{xz}^{\text{linear}}$ (Figure 1), respectively. For example, $p_{s1i}$ is replaced by $N_{s1i}^{\langle1\rangle}$–$N_{s1i}^{\langle4\rangle}$ as follows.

$$\begin{aligned}[p_{s1i}]\Rightarrow N_{s1i}^{\langle1\rangle}+\alpha\Bigg[&\left(\frac{|x|}{L}+\frac{|y|}{W}-\frac{|xy|}{LW}\right)*N_{s1i}^{\langle1\rangle}-\frac{1}{L}\left(1-\frac{|y|}{W}\right)*N_{s1i}^{\langle2\rangle}\\&-\frac{1}{W}\left(1-\frac{|x|}{L}\right)*N_{s1i}^{\langle3\rangle}-\frac{1}{LW}*N_{s1i}^{\langle4\rangle}\Bigg]\end{aligned} \tag{3}$$

Similarly, the solutions under parabolic loading conditions can also be expressed as Equations (A1)–(A6), except for the integral functions. Hence, only the stress integral functions are presented.

$$N_{s1i}^{\langle1\rangle}=S_1-S_2 \tag{4}$$

$$N_{s1i}^{\langle2\rangle}=-yS_3+y^*S_4-z_iS_5 \tag{5}$$

$$N_{s1i}^{\langle3\rangle}=-(R_i-R_{x^*i}-R_{y^*i}+R_{x^*y^*i}) \tag{6}$$

$$N_{s1i}^{\langle4\rangle}=-\tfrac{1}{2}[(R_i-R_{y^*i})x-(R_{x^*i}-R_{x^*y^*i})x^*+(y^2+z_i^2)S_3-(y^{*^2}+z_i^2)S_4] \tag{7}$$

$$N_{s2i}^{\langle1\rangle}=S_3-S_4 \tag{8}$$

$$N_{s2i}^{\langle2\rangle}=N_{s1i}^{\langle3\rangle} \tag{9}$$

$$N_{s2i}^{\langle3\rangle}=-xS_1+x^*S_2-z_iS_5 \tag{10}$$

$$N_{s2i}^{\langle4\rangle}=-\tfrac{1}{2}[(R_i-R_{x^*i})y-(R_{y^*i}-R_{x^*y^*i})y^*+(x^2+z_i^2)S_1-(x^{*^2}+z_i^2)S_2] \tag{11}$$

$$N_{s3i}^{\langle1\rangle}=S_5 \tag{12}$$

 

$$N_{s3i}^{\langle 2\rangle} = z_i N_{s1i}^{\langle 1\rangle} \tag{13}$$

$$N_{s3i}^{\langle 3\rangle} = \text{switch } x, y \text{ in } N_{s3i}^{\langle 2\rangle} \tag{14}$$

$$N_{s3i}^{\langle 4\rangle} = z_i N_{s1i}^{\langle 3\rangle} \tag{15}$$

$$N_{s4i}^{\langle 1\rangle} = S_6 - S_7 \tag{16}$$

$$N_{s4i}^{\langle 2\rangle} = -yS_8 + y^* S_9 - z_i N_{s2i}^{\langle 1\rangle} \tag{17}$$

$$N_{s4i}^{\langle 3\rangle} = \text{switch } x, y \text{ in } N_{s4i}^{\langle 2\rangle} \tag{18}$$

$$N_{s4i}^{\langle 4\rangle} = -\tfrac{1}{2}(LW + x^2 S_{10} - x^{*^2} S_{11} + y^2 S_8 - y^{*^2} S_9 - z_i^2 S_5) \tag{19}$$

$$N_{s5i}^{\langle 1\rangle} = S_5 + S_8 - S_9 \tag{20}$$

$$N_{s5i}^{\langle 2\rangle} = yS_{12} - y^* S_{13} + z_i N_{s1i}^{\langle 1\rangle} \tag{21}$$

$$N_{s5i}^{\langle 3\rangle} = -xS_6 + x^* S_7 \tag{22}$$

$$N_{s5i}^{\langle 4\rangle} = \tfrac{1}{2}(z_i N_{s1i}^{\langle 3\rangle} - x^2 S_6 + x^{*^2} S_7 + y^2 S_{12} - y^{*^2} S_{13}) \tag{23}$$

$$N_{s6i}^{\langle 1\rangle} = N_{s3i}^{\langle 1\rangle} - N_{s5i}^{\langle 1\rangle} \tag{24}$$

$$N_{s6i}^{\langle 2\rangle} = N_{s3i}^{\langle 2\rangle} - N_{s5i}^{\langle 2\rangle} \tag{25}$$

$$N_{s6i}^{\langle 3\rangle} = N_{s3i}^{\langle 3\rangle} - N_{s5i}^{\langle 3\rangle} \tag{26}$$

$$N_{s6i}^{\langle 4\rangle} = N_{s3i}^{\langle 4\rangle} - N_{s5i}^{\langle 4\rangle} \tag{27}$$

$$N_{s7i}^{\langle 1\rangle} = -y\left(\frac{1}{R_i + z_i} - \frac{1}{R_{x^*i} + z_i}\right) + y^*\left(\frac{1}{R_{y^*i} + z_i} - \frac{1}{R_{x^*y^*i} + z_i}\right) \tag{28}$$

$$\begin{aligned} N_{s7i}^{\langle 2\rangle} = &- y\left(\frac{x}{R_i + z_i} - \frac{x^*}{R_{x^*i} + z_i}\right) + y^*\left(\frac{x}{R_{y^*i} + z_i} - \frac{x^*}{R_{x^*y^*i} + z_i}\right) \\ &- yS_3 + y^* S_4 + z_i(S_8 - S_9) \end{aligned} \tag{29}$$

$$N_{s7i}^{\langle 3\rangle} = x^2\left(\frac{1}{R_i + z_i} - \frac{1}{R_{y^*i} + z_i}\right) - x^{*^2}\left(\frac{1}{R_{x^*i} + z_i} - \frac{1}{R_{x^*y^*i} + z_i}\right) + z_i(S_6 - S_7) \tag{30}$$

$$\begin{aligned} N_{s7i}^{\langle 4\rangle} = &- \frac{x}{2}(R_i - R_{y^*i}) + \frac{x^*}{2}(R_{x^*i} - R_{x^*y^*i}) \\ &+ x^3\left(\frac{1}{R_i + z_i} - \frac{1}{R_{y^*i} + z_i}\right) - x^{*^3}\left(\frac{1}{R_{x^*i} + z_i} - \frac{1}{R_{x^*y^*i} + z_i}\right) \\ &- \frac{(y^2 + z_i^2)}{2} S_3 + \frac{(y^{*^2} + z_i^2)}{2} S_4 \end{aligned} \tag{31}$$

 

$$N_{s8i}^{\langle 1\rangle} = \text{switch } x, y \text{ in } N_{s7i}^{\langle 1\rangle} \tag{32}$$

$$N_{s8i}^{\langle 2\rangle} = \text{switch } x, y \text{ in } N_{s7i}^{\langle 3\rangle} \tag{33}$$

$$N_{s8i}^{\langle 3\rangle} = \text{switch } x, y \text{ in } N_{s7i}^{\langle 2\rangle} \tag{34}$$

$$N_{s8i}^{\langle 4\rangle} = \text{switch } x, y \text{ in } N_{s7i}^{\langle 4\rangle} \tag{35}$$

where

$$x^* = x - L, \quad y^* = y - W, \quad R_{x^*i} = \sqrt{x^{*^2} + y^2 + z_i^2}, \quad R_{y^*i} = \sqrt{x^2 + y^{*^2} + z_i^2}$$

$$R_{x^*y^*i} = \sqrt{x^{*^2} + y^{*^2} + z_i^2} \ (i = 1, 2, 3, a, b, c, d, e);$$

$$S_1 = \ln\left|\frac{R_{y^*i} + y^*}{R_i + y}\right|, \quad S_2 = \ln\left|\frac{R_{x^*y^*i} + y^*}{R_{x^*i} + y}\right|$$

$$S_3 = \left|\frac{R_{x^*i} + x^*}{R_i + x}\right|, \quad S_4 = \ln\left|\frac{R_{x^*y^*i} + x^*}{R_{y^*i} + x}\right|,$$

$$S_5 = \tan^{-1}\frac{xy}{z_i R_i} - \tan^{-1}\frac{x^*y}{z_i R_{x^*i}} - \tan^{-1}\frac{xy^*}{z_i R_{y^*i}} + \tan^{-1}\frac{x^*y^*}{z_i R_{x^*y^*i}}$$

$$S_6 = \ln\left|\frac{R_{y^*i} + z_i}{R_i + z_i}\right|, \quad S_7 = \ln\left|\frac{R_{x^*y^*i} + z_i}{R_{x^*i} + z_i}\right|,$$

$$S_8 = \tan^{-1}\frac{y^2 + z_i(R_i + z_i)}{xy} - \tan^{-1}\frac{y^2 + z_i(R_{x^*i} + z_i)}{x^*y}$$

$$S_9 = \tan^{-1}\frac{y^{*^2} + z_i(R_{y^*i} + z_i)}{xy^*} - \tan^{-1}\frac{y^{*^2} + z_i(R_{x^*y^*i} + z_i)}{x^*y^*}$$

$$S_{10} = \tan^{-1}\frac{x^2 + z_i(R_i + z_i)}{xy} - \tan^{-1}\frac{x^2 + z_i(R_{y^*i} + z_i)}{xy^*}$$

$$S_{11} = \tan^{-1}\frac{x^{*^2} + z_i(R_{x^*i} + z_i)}{x^*y} - \tan^{-1}\frac{x^{*^2} + z_i(R_{x^*y^*i} + z_i)}{x^*y^*},$$

$$S_{12} = \ln\left|\frac{R_{x^*i} + z_i}{R_i + z_i}\right|, \quad S_{13} = \ln\left|\frac{R_{x^*y^*i} + z_i}{R_{y^*i} + z_i}\right|$$

Equations (A1)–(A6), (3) and (4)–(35) can easily be solved automatically to calculate the stresses in a transversely isotropic half-space subjected to three-dimensional, buried, linearly varying rectangular loads.

### 2.2. *Parabolic rectangular loads*

A non-linear, three-dimensional, buried load distributed as a concave parabola on a rectangle (Figure 3) is considered to demonstrate the results for non-linearly distributed loads. Figure 3 depicts that the concave parabolic load applied over a rectangular region with sides $L$ and $W$.

 

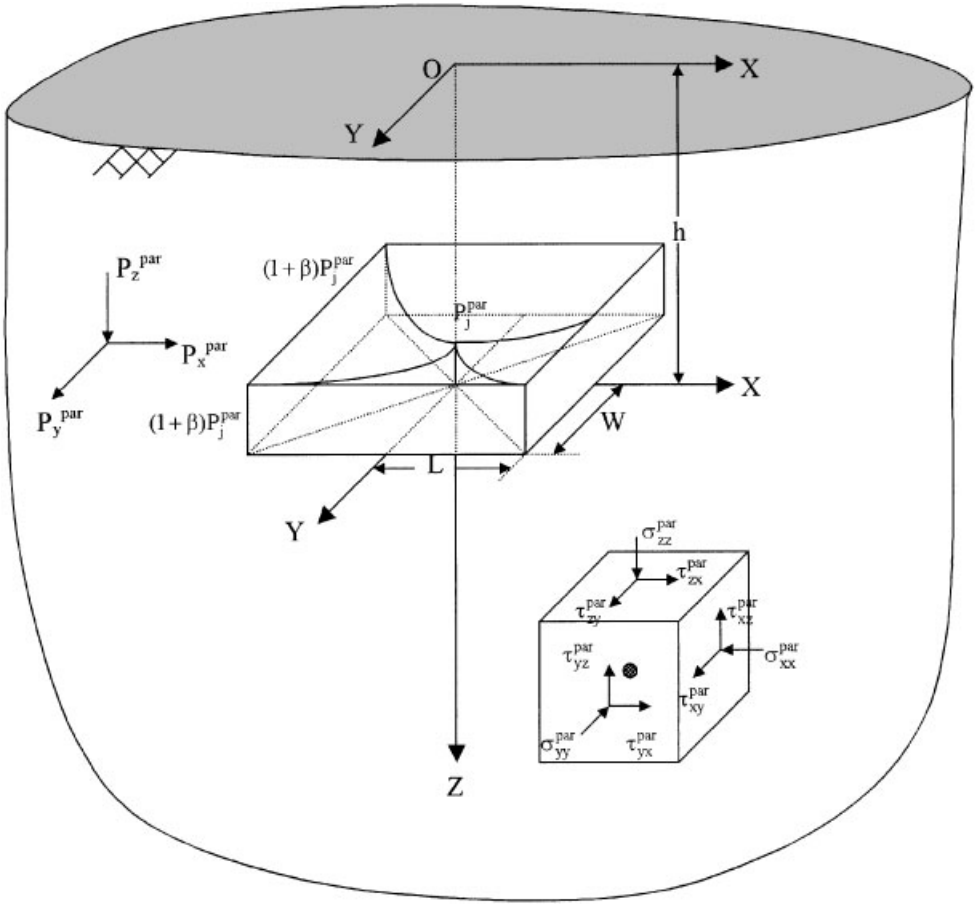


Figure 3. The case of concave parabolic rectangular loads with $L*W$ area at the buried depth of $h(\beta > 0)$.

The type of loading shown in Figure 3 has the following form [14]:

$$\tilde{P}_j^{\text{par}} = P_j^{\text{par}}\left[1+\beta\left(\frac{x^2}{L^2}+\frac{y^2}{W^2}-\frac{x^2y^2}{L^2W^2}\right)\right] \tag{36}$$

where $\beta$ is a constant, and that specifies the following three cases:

*Case* 1: $\beta > 0$, the load is concave parabolic, as shown in Figure 3;

*Case* 2: $\beta = 0$, the load is uniform; this case is identical to that of $\alpha = 0$ (Figure 2(a));

*Case* 3: $\beta < 0$, the load is convex parabolic. Figure 4 depicts zero contact stress at the region shown at the edges of Figure 3, for the case of $\beta = -1$.

The elementary force $P_j$, acting on a small rectangle, can also be expressed as $\tilde{P}_j^{\text{par}}\,\mathrm{d}\zeta\,\mathrm{d}\eta$ $(j = x, y, z)$ (forces per unit area). Similarly, as for the linearly varying rectangular load, the solutions for stresses can be obtained by direct integration as follows:

$$[\sigma]^{\text{par}} = \int_0^L \int_0^W [\sigma]^p \,\mathrm{d}\eta\,\mathrm{d}\varsigma \tag{37}$$

 

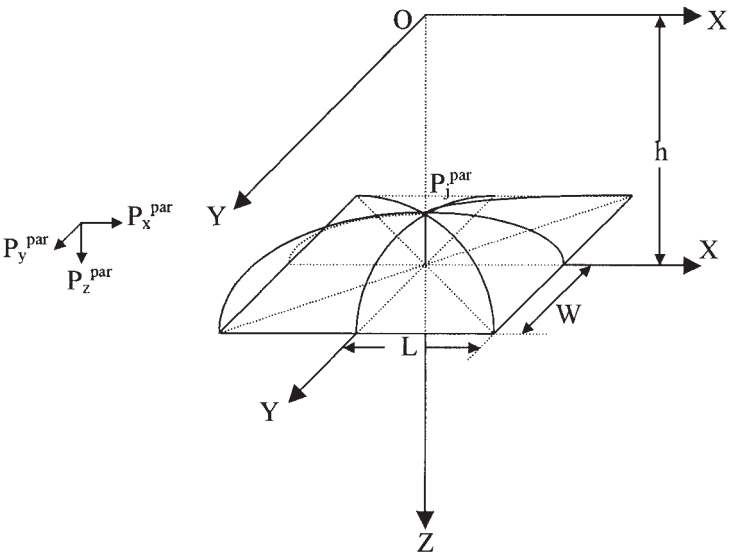


Figure 4. The case of completely convex parabolic rectangular loads with $L*W$ area at the buried depth of $h(\beta = -1)$.

where the superscripts, par and $p$, refer to the stress components that are induced by a parabolic load and a point load, respectively. The explicit solutions for stresses in a half-space can be regrouped in the forms of Equations (A1)–(A6). The exact solutions in this case are the same as Equations (A1)–(A6), except that the stress elementary functions $p_{s1i}$, $p_{s2i}, \ldots, p_{s8i}$ are replaced by the stress integral functions, $N_{s1i}^{\langle 1\rangle}$–$N_{s1i}^{\langle 9\rangle}$, $N_{s2i}^{\langle 1\rangle}$– $N_{s2i}^{\langle 9\rangle}, \ldots, N_{s8i}^{\langle 1\rangle}$–$N_{s8i}^{\langle 9\rangle}$ $(i = 1, 2, 3, a, b, c, d, e)$ for $\sigma_{xx}^{\text{par}}$, $\sigma_{yy}^{\text{par}}, \sigma_{zz}^{\text{par}}, \tau_{xy}^{\text{par}}$, $\tau_{yz}^{\text{par}}, \tau_{xz}^{\text{par}}$ (Figure 3), respectively. In this loading case, for instance, $p_{s1i}$ should be replaced by $N_{s1i}^{\langle 1\rangle}$–$N_{s1i}^{\langle 9\rangle}$ as follows:

$$
\begin{aligned}
[p_{s1i}] \Rightarrow N_{s1i}^{\langle 1\rangle} + \beta\Bigg[ & \left(\frac{x^2}{L^2} + \frac{y^2}{W^2} * S_{14}\right) * N_{s1i}^{\langle 1\rangle} \\
& - \frac{2x}{L^2} * S_{15} * N_{s1i}^{\langle 2\rangle} - \frac{2y}{W^2} * S_{14} * N_{s1i}^{\langle 3\rangle} - \frac{4xy}{L^2W^2} * N_{s1i}^{\langle 4\rangle} \\
& + \frac{S_{15}}{L^2} * N_{s1i}^{\langle 5\rangle} + \frac{S_{14}}{W^2} * N_{s1i}^{\langle 6\rangle} + \frac{1}{L^2W^2}(2x * N_{s1i}^{\langle 7\rangle} + 2y * N_{s1i}^{\langle 8\rangle} - N_{s1i}^{\langle 9\rangle})\Bigg]
\end{aligned} \tag{38}
$$

where $S_{14} = 1 - \frac{x^2}{L^2}$, $S_{15} = 1 - \frac{y^2}{W^2}$. Equations (4)–(35) are the stress integral functions for $N_{s1i}^{\langle 1\rangle}$–$N_{s1i}^{\langle 4\rangle}$, $N_{s2i}^{\langle 1\rangle}$–$N_{s2i}^{\langle 4\rangle}, \ldots, N_{s8i}^{\langle 1\rangle}$–$N_{s8i}^{\langle 4\rangle}$. Hence, only the integral functions for $N_{s1i}^{\langle 5\rangle}$–$N_{s1i}^{\langle 9\rangle}$, $N_{s2i}^{\langle 5\rangle}$–$N_{s2i}^{\langle 9\rangle}, \ldots, N_{s8i}^{\langle 5\rangle}$–$N_{s8i}^{\langle 9\rangle}$ are given as follows:

$$
N_{s1i}^{\langle 5\rangle} = (R_i - R_{x^*i})y - (R_{y^*i} - R_{x^*y^*i})y^* - z_i^2 N_{s1i}^{\langle 1\rangle} \tag{39}
$$

$$
N_{s1i}^{\langle 6\rangle} = N_{s2i}^{\langle 4\rangle} \tag{40}
$$

 

$$N_{s1i}^{\langle 7\rangle} = -\tfrac{1}{3}[(yR_i - y^*R_{y^*i})x - (yR_{x^*i} - y^*R_{x^*y^*i})x^* + x^3S_1 - x^{*^3}S_2 + y^3S_3 - y^{*^3}S_4 - z_i^3S_5] \tag{41}$$

$$N_{s1i}^{\langle 8\rangle} = -\frac{(x^2 - 2y^2 - 2z_i^2)}{3}R_i + \frac{(x^{*^2} - 2y^2 - 2z_i^2)}{3}R_{x^*i} + \frac{(x^2 - 2y^{*^2} - 2z_i^2)}{3}R_{y^*i} - \frac{(x^{*^2} - 2y^{*^2} - 2z_i^2)}{3}R_{x^*y^*i} \tag{42}$$

$$N_{s1i}^{\langle 9\rangle} = -\tfrac{1}{4}\{[(x^2 - 2y^2 - z_i^2)R_i - (x^{*^2} - 2y^2 - z_i^2)R_{x^*i}]y - [(x^2 - 2y^{*^2} - z_i^2)R_{y^*i} - (x^{*^2} - 2y^{*^2} - z_i^2)R_{x^*y^*i}]y^* + (x^4 - z_i^4)S_1 - (x^{*^4} - z_i^4)S_2\} \tag{43}$$

$$N_{s2i}^{\langle 5\rangle} = N_{s1i}^{\langle 4\rangle} \tag{44}$$

$$N_{s2i}^{\langle 6\rangle} = (R_i - R_{y^*i})x - (R_{x^*i} - R_{x^*y^*i})x^* - z_i^2N_{s2i}^{\langle 1\rangle} \tag{45}$$

$$N_{s2i}^{\langle 7\rangle} = \text{switch } x, y \text{ in } N_{s1i}^{\langle 8\rangle} \tag{46}$$

$$N_{s2i}^{\langle 8\rangle} = N_{s1i}^{\langle 7\rangle} \tag{47}$$

$$N_{s2i}^{\langle 9\rangle} = \text{switch } x, y \text{ in } N_{s1i}^{\langle 9\rangle} \tag{48}$$

$$N_{s3i}^{\langle 5\rangle} = z_iN_{s1i}^{\langle 2\rangle} \tag{49}$$

$$N_{s3i}^{\langle 6\rangle} = \text{switch } x, y \text{ in } N_{s3i}^{\langle 5\rangle} \tag{50}$$

$$N_{s3i}^{\langle 7\rangle} = z_iN_{s1i}^{\langle 6\rangle} \tag{51}$$

$$N_{s3i}^{\langle 8\rangle} = \text{switch } x, y \text{ in } N_{s3i}^{\langle 7\rangle} \tag{52}$$

$$N_{s3i}^{\langle 9\rangle} = z_iN_{s1i}^{\langle 7\rangle} \tag{53}$$

$$N_{s4i}^{\langle 5\rangle} = -z_iN_{s1i}^{\langle 3\rangle} - y^2S_{12} + y^{*^2}S_{13} \tag{54}$$

$$N_{s4i}^{\langle 6\rangle} = \text{switch } x, y \text{ in } N_{s4i}^{\langle 5\rangle} \tag{55}$$

$$N_{s4i}^{\langle 7\rangle} = -\frac{LW(y + y^*)}{3} + \frac{z_i}{3}[(R_i - R_{y^*i})x - (R_{x^*i} - R_{x^*y^*i})x^*] - \tfrac{2}{3}(x^3S_6 - x^{*^3}S_7) - \tfrac{1}{3}(y^3S_8 - y^{*^3}S_9) + \frac{z_i^3}{3}(S_3 - S_4) \tag{56}$$

$$N_{s4i}^{\langle 8\rangle} = \text{switch } x, y \text{ in } N_{s4i}^{\langle 7\rangle} \tag{57}$$

 

$$N_{s4i}^{\langle 9\rangle} = -\frac{LW(x+x^*)(y+y^*)}{4} - \tfrac{1}{2}(x^4 S_6 - x^{*^4} S_7 + y^4 S_{12} - y^{*^4} S_{13}) + \frac{z_i}{6}[(x^2+y^2-2z_i^2)R_i - (x^{*^2}+y^2-2z_i^2)R_{x^*i} - (x^2+y^{*^2}-2z_i^2)R_{y^*i} - (x^{*^2}+y^{*^2}-2z_i^2)R_{x^*y^*i}] \tag{58}$$

$$N_{s5i}^{\langle 5\rangle} = -LW - y^2 S_8 + y^{*^2} S_9 - 2z_i(yS_3 - y^* S_4) - z_i^2 S_5 \tag{59}$$

$$N_{s5i}^{\langle 6\rangle} = LW + x^2 S_{10} - x^{*^2} S_{11} + z_i(xS_1 - x^* S_2) \tag{60}$$

$$N_{s5i}^{\langle 7\rangle} = \frac{2LW(x+x^*)}{3} + \tfrac{2}{3}(x^3 S_{10} - x^{*^3} S_{11}) + \tfrac{1}{3}(y^3 S_{12} - y^{*^3} S_{13}) - \frac{z_i}{6}[(R_i - R_{x^*i})y - (R_{y^*i} - R_{x^*y^*i})y^* - (3x^2 - z_i^2)S_1 + (3x^{*^2} - z_i^2)S_2] \tag{61}$$

$$N_{s5i}^{\langle 8\rangle} = -\frac{2LW(x+x^*)}{3} - \tfrac{1}{3}(x^3 S_6 - x^{*^3} S_7) - \tfrac{2}{3}(y^3 S_8 - y^{*^3} S_9) - \frac{z_i}{3}[(R_i - R_{y^*i})x - (R_{x^*i} - R_{x^*y^*i})x^* + (3y^2 + z_i^2)S_3 - (3y^{*^2} + z_i^2)S_4] \tag{62}$$

$$N_{s5i}^{\langle 9\rangle} = \frac{LW(x^2 + xx^* + x^{*^2} - y^2 - yy^* - y^{*^2})}{2} + \tfrac{1}{2}(x^4 S_{10} - x^{*^4} S_{11} - y^4 S_8 + y^{*^4} S_9) - \frac{z_i}{6}[(yR_i - y^* R_{y^*i})x - (yR_{x^*i} - y^* R_{x^*y^*i})x^*] + \frac{z_i}{3}\left(x^3 S_1 - x^{*^3} S_2 - 2y^3 S_3 + 2y^{*^3} S_4 + \frac{z_i^3}{2} S_5\right) \tag{63}$$

$$N_{s6i}^{\langle 5\rangle} = N_{s3i}^{\langle 5\rangle} - N_{s5i}^{\langle 5\rangle} \tag{64}$$

$$N_{s6i}^{\langle 6\rangle} = N_{s3i}^{\langle 6\rangle} - N_{s5i}^{\langle 6\rangle} \tag{65}$$

$$N_{s6i}^{\langle 7\rangle} = N_{s3i}^{\langle 7\rangle} - N_{s5i}^{\langle 7\rangle} \tag{66}$$

$$N_{s6i}^{\langle 8\rangle} = N_{s3i}^{\langle 8\rangle} - N_{s5i}^{\langle 8\rangle} \tag{67}$$

$$N_{s6i}^{\langle 9\rangle} = N_{s3i}^{\langle 9\rangle} - N_{s5i}^{\langle 9\rangle} \tag{68}$$

$$N_{s7i}^{\langle 5\rangle} = y\left[R_i - R_{x^*i} + y^2\left(\frac{1}{R_i + z_i} - \frac{1}{R_{x^*i} + z_i}\right)\right] - y^*\left[R_{y^*i} - R_{x^*y^*i} + y^{*^2}\left(\frac{1}{R_{y^*i} + z_i} - \frac{1}{R_{x^*y^*i} + z_i}\right)\right] + 2z_i(yS_{12} - y^* S_{13}) \tag{69}$$

 

$$N_{s7i}^{\langle 6\rangle} = y\left(\frac{x^2}{R_i+z_i}-\frac{x^{*^2}}{R_{x^*i}+z_i}\right) - y^*\left(\frac{x^2}{R_{y^*i}+z_i}-\frac{x^{*^2}}{R_{x^*y^*i}+z_i}\right) + (x^2-z_i^2)S_1 - (x^{*^2}-z_i^2)S_2 - 2z_i(xS_{10}-x^*S_{11}) \tag{70}$$

$$N_{s7i}^{\langle 7\rangle} = -\frac{y}{3}(xR_i - x^*R_{x^*i}) + \frac{y^*}{3}(xR_{y^*i} - x^*R_{x^*y^*i}) + y\left(\frac{x^3}{R_i+z_i}-\frac{x^{*^3}}{R_{x^*i}+z_i}\right) - y^*\left(\frac{x^3}{R_{y^*i}+z_i}-\frac{x^{*^3}}{R_{x^*y^*i}+z_i}\right) + \tfrac{1}{3}(2x^3S_1 - 2x^{*^3}S_2 - y^3S_3 + y^{*^3}S_4 + z_i^3S_5) - z_i(x^2S_{10} - x^{*^2}S_{11}) \tag{71}$$

$$N_{s7i}^{\langle 8\rangle} = \tfrac{1}{3}(R_i^3 - R_{x^*i}^3 - R_{y^*i}^3 + R_{x^*y^*i}^3) + y^4\left(\frac{1}{R_i+z_i}-\frac{1}{R_{x^*i}+z_i}\right) - y^{*^4}\left(\frac{1}{R_{y^*i}+z_i}-\frac{1}{R_{x^*y^*i}+z_i}\right) + z_i(y^2S_{12} - y^{*^2}S_{13}) \tag{72}$$

$$N_{s7i}^{\langle 9\rangle} = -\frac{2LWz_i(x+x^*)}{3} + \tfrac{1}{2}[y(x^2R_i - x^{*^2}R_{x^*i}) - y^*(x^2R_{y^*i} - x^{*^2}R_{x^*y^*i})] + \tfrac{1}{6}[(3x^4+z_i^4)S_1 - (3x^{*^4}+z_i^4)S_2] + y^5\left(\frac{1}{R_i+z_i}-\frac{1}{R_{x^*i}+z_i}\right) - y^{*^5}\left(\frac{1}{R_{y^*i}+z_i}-\frac{1}{R_{x^*y^*i}+z_i}\right) - \frac{2z_i}{3}(x^3S_{10} - x^{*^3}S_{11} - y^3S_{12} + y^{*^3}S_{13}) + \frac{z_i^2}{6}[y(R_i - R_{x^*i}) - y^*(R_{y^*i} - R_{x^*y^*i})] \tag{73}$$

$$N_{s8i}^{\langle 5\rangle} = \text{switch } x, y \text{ in } N_{s7i}^{\langle 6\rangle} \tag{74}$$

$$N_{s8i}^{\langle 6\rangle} = \text{switch } x, y \text{ in } N_{s7i}^{\langle 5\rangle} \tag{75}$$

$$N_{s8i}^{\langle 7\rangle} = \text{switch } x, y \text{ in } N_{s7i}^{\langle 8\rangle} \tag{76}$$

$$N_{s8i}^{\langle 8\rangle} = \text{switch } x, y \text{ in } N_{s7i}^{\langle 7\rangle} \tag{77}$$

$$N_{s8i}^{\langle 9\rangle} = \text{switch } x, y \text{ in } N_{s7i}^{\langle 9\rangle} \tag{78}$$

Equations (A1)–(A6), (4)–(35), (38), and (39)–(78) can be applied to compute the stresses in a transversely isotropic half-space subjected to three-dimensional, buried and parabolic rectangular loads. Also, the presented formulae for stresses are consistent with those presented by Teferra and Schultze [11] as the medium is isotropic and is in a state of plane strain. Moreover, stresses in the media in response to non-uniform, irregularly shaped loads can be estimated by superposing values that correspond to the rectangular sub-areas. Figure 5 shows a

 

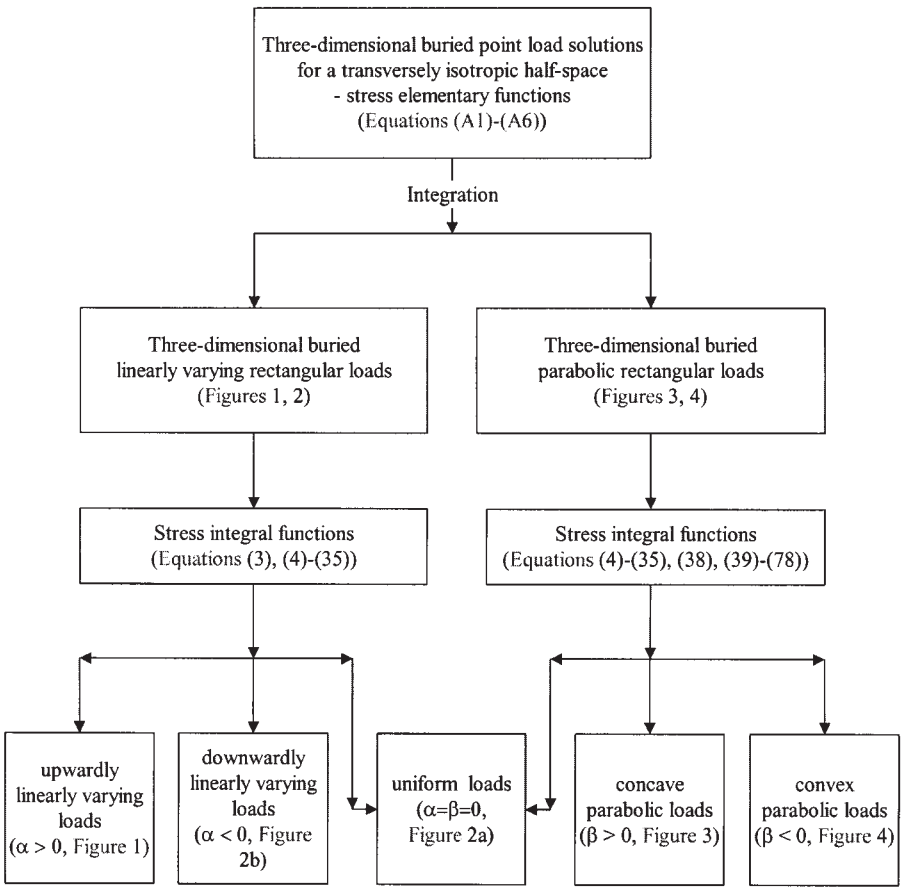


Figure 5. Flow chart to compute the stresses in a transversely isotropic half-space subjected to presented loading types.

flow chart of the computation for stresses induced by linearly varying, uniform, and parabolic rectangular loads in a transversely isotropic half-space.

## 3. ILLUSTRATIVE EXAMPLE

This section presents a parametric study to confirm the derived solutions and elucidate the effect of the type and degree of material anisotropy, the dimensions of the loaded area, and the types of loading on the stresses. An example illustrates the solution of the vertical stress, as depicted in Figures 6–11, for the action of vertical, linearly varying, uniform and parabolic loads on a rectangle. Several types of isotropic and transversely isotropic rocks are considered as foundation materials. Table I lists their elastic properties, with $E/E'$ and $G/G'$ ranging between 1 and 3 and $v/v'$ varying between 0.75 and 1.5. The values of $E$ and $v$ adopted in Table I are 50 GPa and 0.25, respectively. The selected domains of anisotropic variation follow the

 

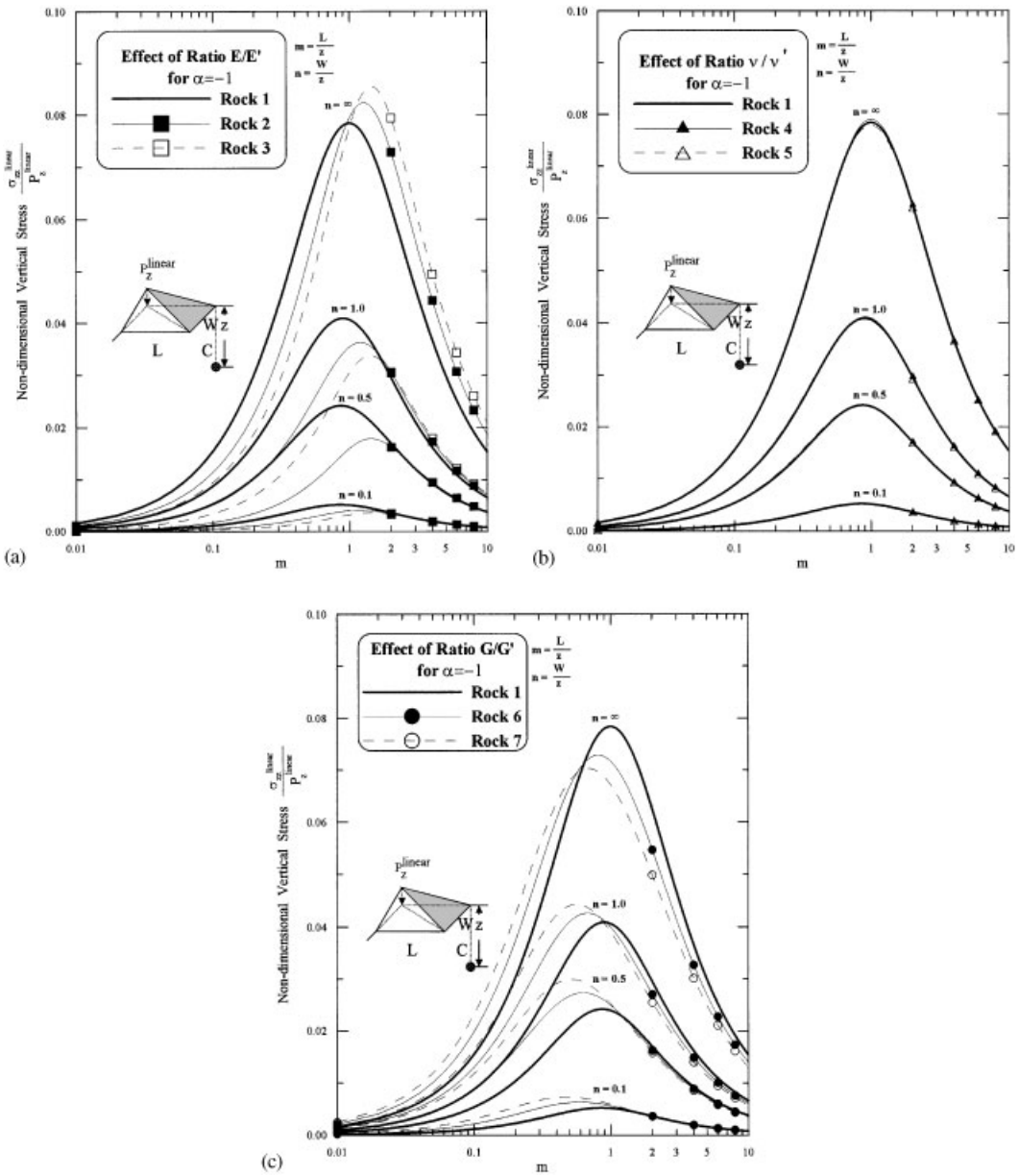


Figure 6. Effect of the type and degree of rock anisotropy on vertical stress induced by the loading case of $\alpha = -1$: (a) for Rocks 1, 2, 3 with $E/E' = 1, 2, 3$, and $\nu/\nu' = G/G' = 1$, respectively; (b) for Rocks 1, 4, 5 with $\nu/\nu' = 1, 0.75, 1.5$, and $E/E' = G/G' = 1$, respectively; (c) for Rocks 1, 6, 7 with $G/G' = 1, 2, 3$, and $E/E' = \nu/\nu' = 1$, respectively.

 

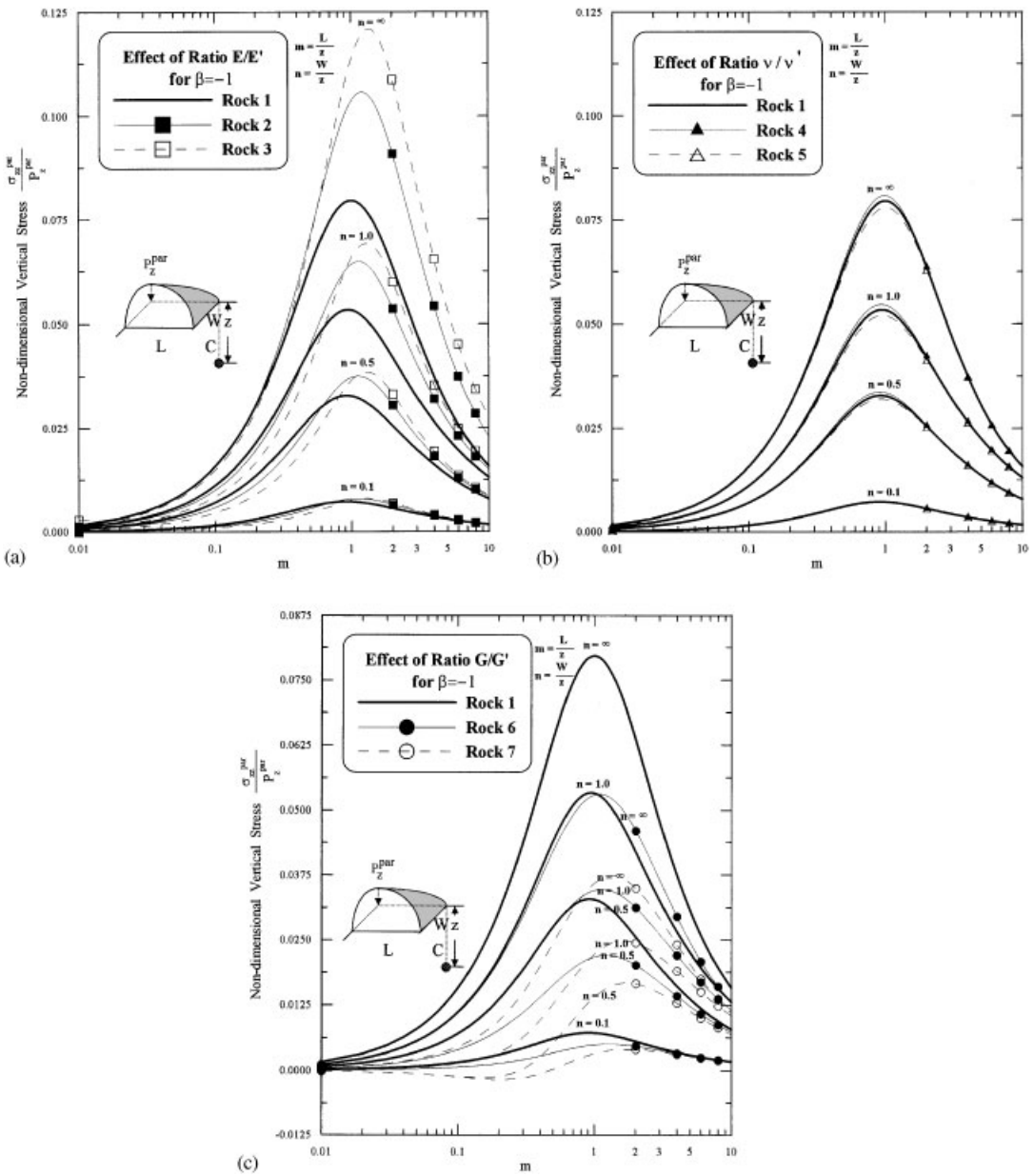


Figure 7. Effect of the type and degree of rock anisotropy on vertical stress induced by the loading case of $\beta = -1$: (a) for Rocks 1, 2, 3 with $E/E' = 1, 2, 3$, and $\nu/\nu' = G/G' = 1$, respectively; (b) for Rocks 1, 4, 5 with $\nu/\nu' = 1, 0.75, 1.5$, and $E/E' = G/G' = 1$, respectively; (c) for Rocks 1, 6, 7 with $G/G' = 1, 2, 3$, and $E/E' = \nu/\nu' = 1$, respectively.

 

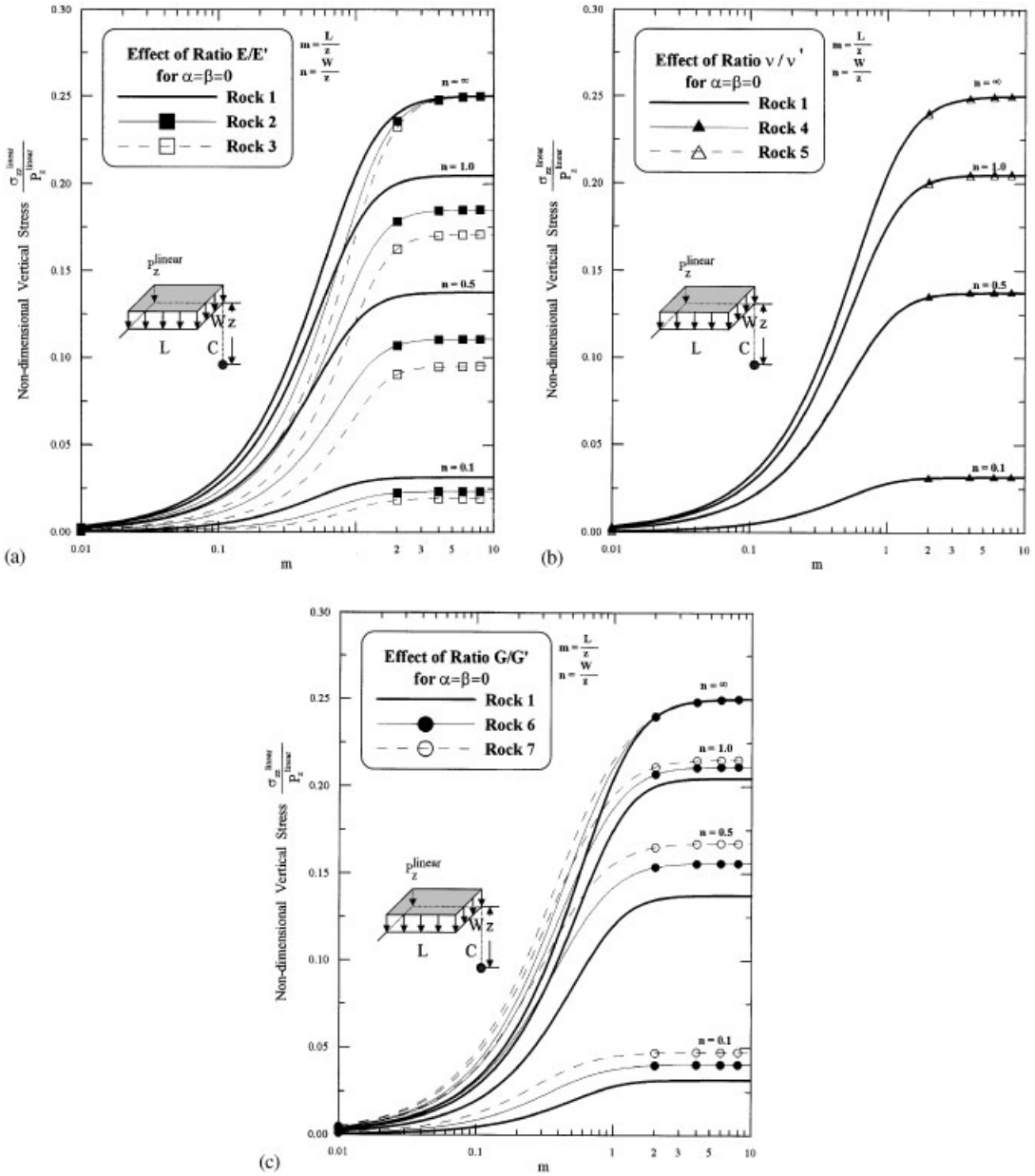


Figure 8. Effect of the type and degree of rock anisotropy on vertical stress induced by the loading case of $\alpha = \beta = 0$: (a) for Rocks 1, 2, 3 with $E/E' = 1, 2, 3$, and $\nu/\nu' = G/G' = 1$, respectively; (b) for Rocks 1, 4, 5 with $\nu/\nu' = 1, 0.75, 1.5$, and $E/E' = G/G' = 1$, respectively; (c) for Rocks 1, 6, 7 with $G/G' = 1, 2, 3$, and $E/E' = \nu/\nu' = 1$, respectively

 

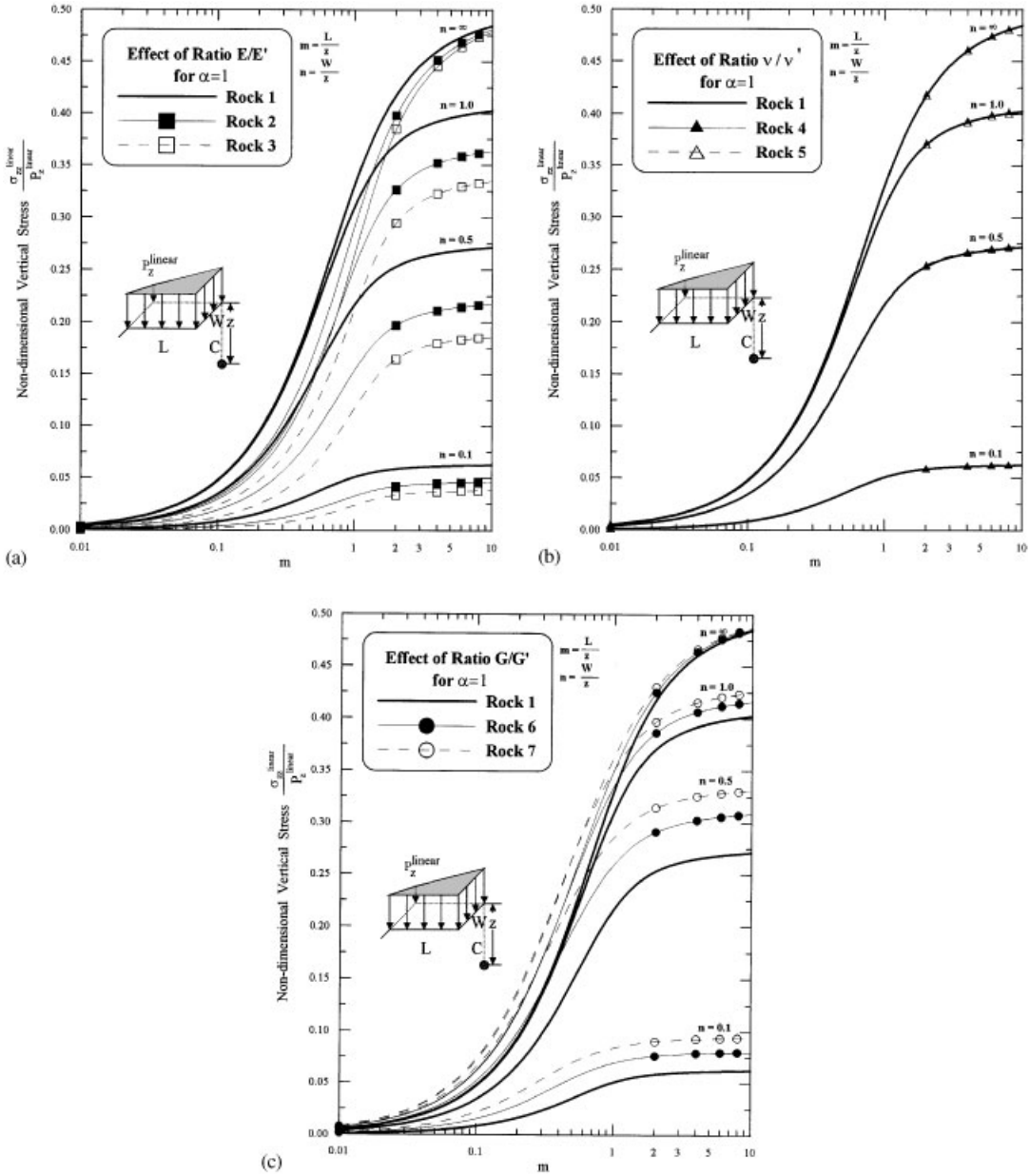


Figure 9. Effect of the type and degree of rock anisotropy on vertical stress induced by the loading case of $\alpha = 1$: (a) for Rocks 1, 2, 3 with $E/E' = 1, 2, 3$, and $\nu/\nu' = G/G' = 1$, respectively; (b) for Rocks 1, 4, 5 with $\nu/\nu' = 1, 0.75, 1.5$, and $E/E' = G/G' = 1$, respectively; (c) for Rocks 1, 6, 7 with $G/G' = 1, 2, 3$, and $E/E' = \nu/\nu' = 1$, respectively.

 

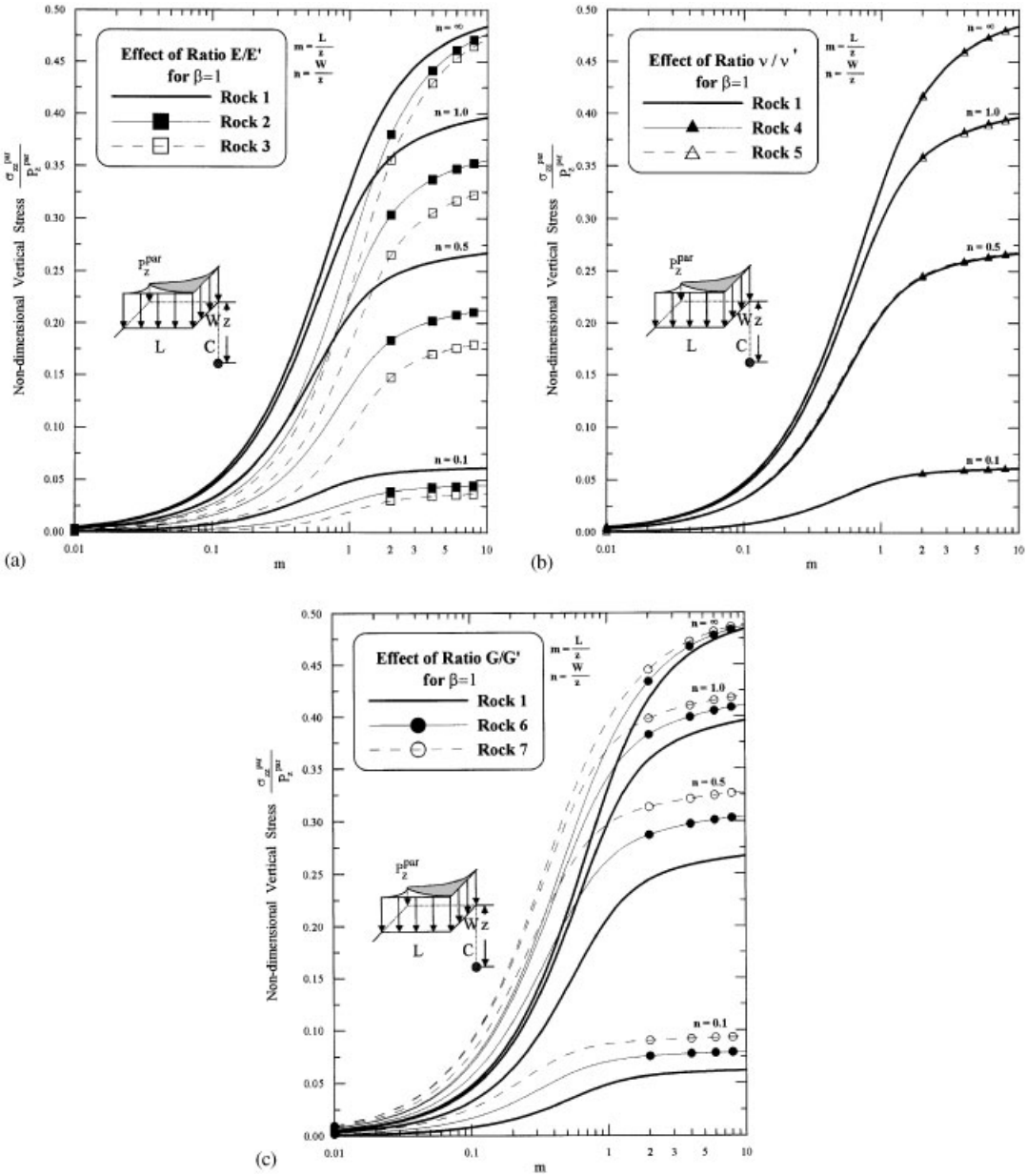


Figure 10. Effect of the type and degree of rock anisotropy on vertical stress induced by the loading case of $\beta = 1$: (a) for Rocks 1, 2, 3 with $E/E' = 1, 2, 3$, and $v/v' = G/G' = 1$, respectively; (b) for Rocks 1, 4, 5 with $v/v' = 1, 0.75$, 1.5, and $E/E' = G/G' = 1$, respectively; (c) for Rocks 1, 6, 7 with $G/G' = 1, 2, 3$, and $E/E' = v/v' = 1$, respectively.

 

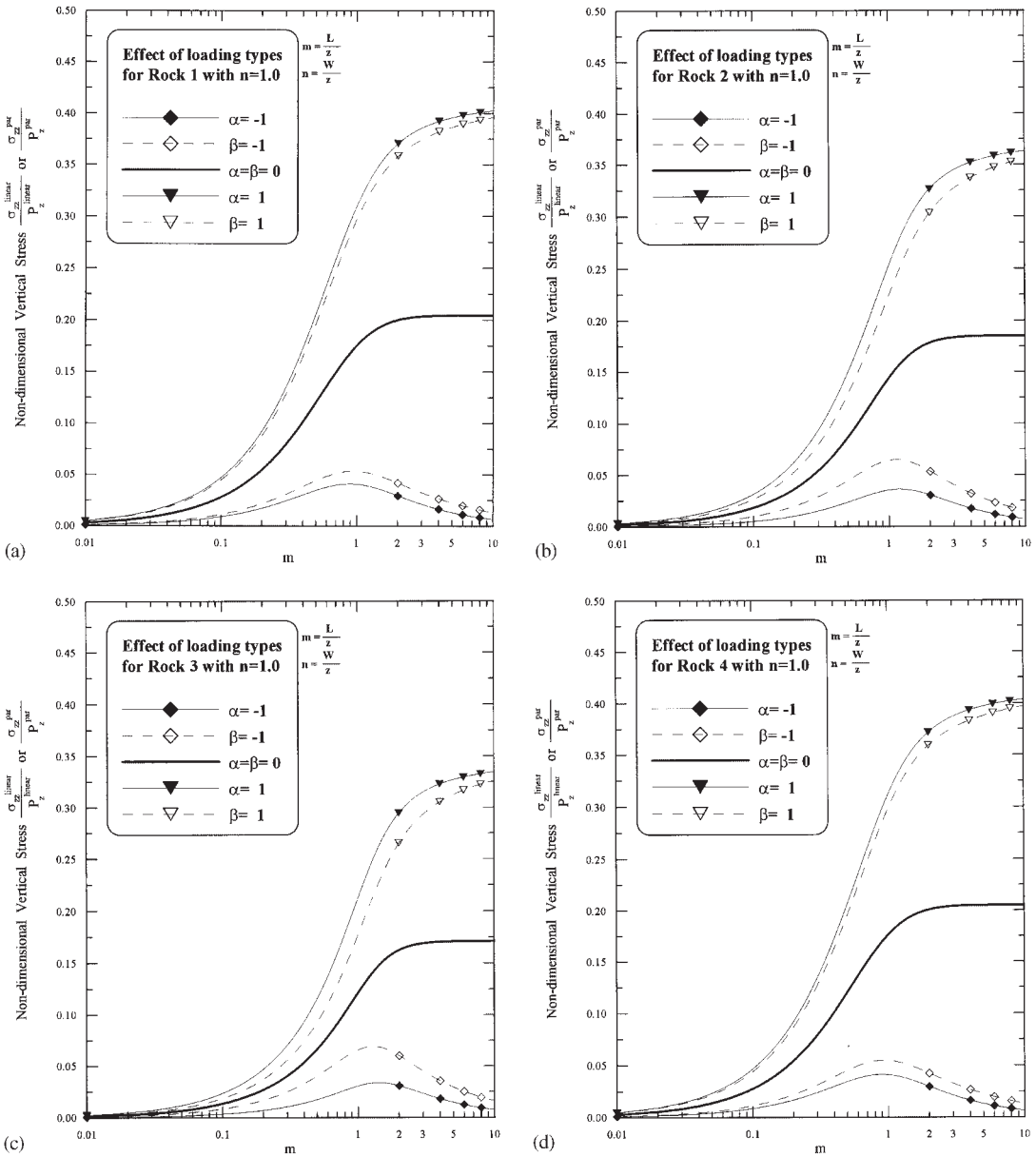


Figure 11. Effect of the presented loading types on vertical stress: (a) for Rock 1 with $E/E' = v/v' = G/G' = 1$; (b) for Rock 2 with $E/E' = 2$, $v/v' = G/G' = 1$; (c) for Rock 3 with $E/E' = 3$, $v/v' = G/G' = 1$; (d) for Rock 4 with $v/v' = 0.75$, $E/E' = G/G' = 1$; (e) for Rock 5 with $v/v' = 1.5$, $E/E' = G/G' = 1$; (f) for Rock 6 with $G/G' = 2$, $E/E' = v/v' = 1$; (g) for Rock 7 with $G/G' = 3$, $E/E' = v/v' = 1$.

suggestions of Gerrard [15] and Amadei *et al.* [16]. The loads act on the horizontal surface ($h = 0$) of isotropic/transversely isotropic rocks in this example. The effect of the degree of anisotropy, specified by the ratios $E/E'$, $v/v'$, and $G/G'$ on the stresses is considered.

 

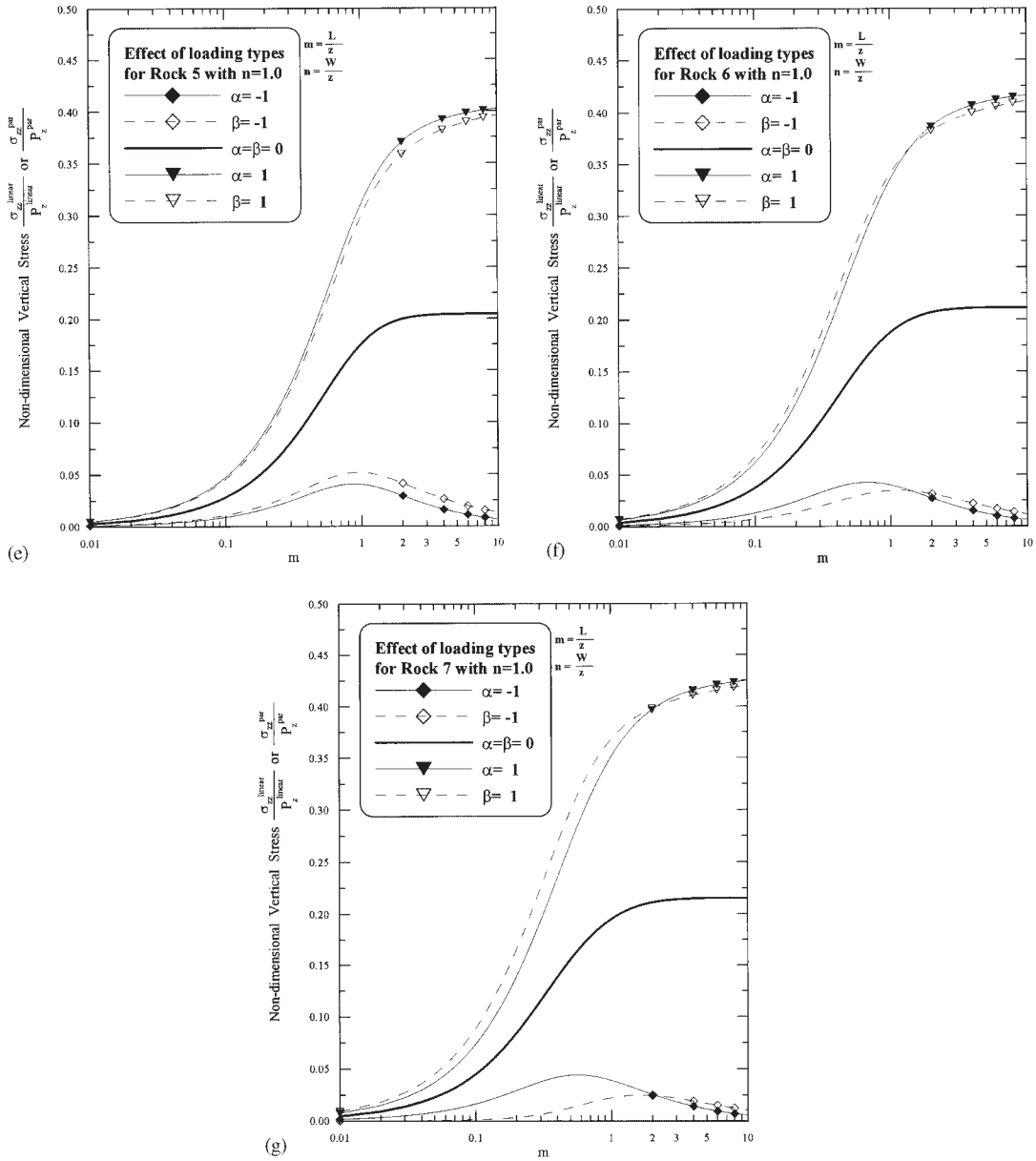


Figure 11. (*continued*)

Using Equations (A1)–(A6), (3), (4)–(35), (38), and (39)–(78), a FORTRAN program was written to calculate the six stress components under linearly varying, uniform and parabolic loading. In this study, only the vertical stress at the right corner, $C$ (at depth $z$ from the surface) of the loaded area was calculated. Figures 6–10 present the normalized vertical stress ($\sigma_{zz}^{\text{linear}}/P_z^{\text{linear}}$ or $\sigma_{zz}^{\text{par}}/P_z^{\text{par}}$) at point $C$, induced by a completely downwardly linearly varying load

 

Table I. Elastic properties and root types for different rocks.

| Rock type | $E/E'$ | $v/v'$ | $G/G'$ | Root type |
|---|---|---|---|---|
| Rock 1. Isotropic | 1.0 | 1.0 | 1.0 | Equal |
| Rock 2. Transversely isotropic | 2.0 | 1.0 | 1.0 | Complex |
| Rock 3. Transversely isotropic | 3.0 | 1.0 | 1.0 | Complex |
| Rock 4. Transversely isotropic | 1.0 | 0.75 | 1.0 | Complex |
| Rock 5. Transversely isotropic | 1.0 | 1.5 | 1.0 | Distinct |
| Rock 6. Transversely isotropic | 1.0 | 1.0 | 2.0 | Distinct |
| Rock 7. Transversely isotropic | 1.0 | 1.0 | 3.0 | Distinct |

($\alpha = -1$), a completely convex parabolic load ($\beta = -1$), a uniform load ($\alpha = \beta = 0$), an upwardly linearly varying load ($\alpha = 1$) and a concave parabolic load ($\beta = 1$), respectively, over a rectangular area for various rock types (Rocks 1–7, Table I) and for various dimensions of the loaded area ($m = L/z$ or $n = W/z$). The figures plot the relationship between two non-dimensional factors, $m$ and $\sigma_{zz}^{\text{linear}}/P_z^{\text{linear}}$ (or $\sigma_{zz}^{\text{par}}/P_z^{\text{par}}$) for $n = 0.1,\ 0.5,\ 1.0,\ \infty$. In these figures, the non-dimensional factor, $n$, is adopted to elucidate the effect of the dimensions of the loaded region on the vertical stress. The stress beneath a strip is that beneath a rectangle as either $L$ or $W$ approaches infinity ($\infty$) [17]. However, practically, a rectangle for which $W/L > 4$ to 5 can be regarded as a strip [18]. In this example, $n = 40$ is selected in the simulation of an infinite load. Hence, with knowledge of the type and magnitude of the loading, the dimensions of the loaded area and the type of rock the vertical stress at point $C$ can be estimated from these figures. Figures 11(a)–11(g) summarize the results of applying the same stress as induced by the loads mentioned above ($\alpha = -1$, $\beta = -1$, $\alpha = \beta = 0$, $\alpha = 1$, $\beta = 1$) to Rocks 1–7, respectively, with $n = 1.0$. With reference to Figures 6–11, the effects of the type and degree of rock anisotropy, loading types and the dimensions of the loaded region on the stress induced by surface loading are investigated below.

Figures 6(a)–6(c), 7(a)–7(c), 8(a)–8(c), 9(a)–9(c), and 10(a)–10(c) plot the vertical stress induced by loading with $\alpha = -1$, $\beta = -1$, $\alpha = \beta = 0$, $\alpha = 1$, and $\beta = 1$ for Rocks 1 ($E/E' = v/v' = G/G' = 1$), 2 ($E/E' = 2, v/v' = G/G' = 1$), 3 ($E/E' = 3, v/v' = G/G' = 1$), Rocks 1, 4 ($v/v' = 0.75, E/E' = G/G' = 1$), 5 ($v/v' = 1.5, E/E' = G/G' = 1$), Rocks 1, 6 ($G/G' = 2, E/E' = v/v' = 1$), 7 ($G/G' = 3, E/E' = v/v' = 1$) with variable non-dimensional factors ($m, n$). From Figure 6(a), the stress induced in Rocks 2 and 3 is less than that in Rock 1 within the smaller loaded region (horizontal scale, $m$); however, the calculated result changes as $m$ increases. For a given $n$ ($= 0.1,\ 0.5,\ 1.0,\ \infty$), the non-dimensional factor, $m$, significantly affects the induced vertical stress at point C. The trend of vertical stress in Figure 6(c) for Rocks 6 and 7 is the opposite of that in Figure 6(a) for Rocks 2 and 3. Figures 6(a) and 6(c) preliminarily imply that the induced stress depends on the type and degree of anisotropy for a given loading ($\alpha = -1$). Figure 7(a) indicates that the induced stress with $\beta = -1$ for Rocks 1–3 increases as $E/E'$ increases, whereas for Rocks 6 and 7 (Figure 7(c)) the results are totally different. Notably, a little of the stress in Figure 7(c) might be transferred by tension in Rock 7, when $n = 0.1$ and 0.5, within a very small loaded area ($m \leqslant 0.5$). Figures 8(a), 9(a) and 10(a) show that for a given loading type ($\alpha = \beta = 0$, $\alpha = 1$, and $\beta = 1$), depth ($z$), and loaded region ($L$ or $W$), the magnitude of the vertical stress decreases as $E/E'$ increases (Rocks 2, 3). Comparing Figures 8(c), 9(c) and 10(c) with Figures 8(a), 9(a) and 10(a) reveals that the non-dimensional vertical stress increases with increases in $G/G'$ (Rocks 6, 7). Figures 6(b), 7(b), 8(b), 9(b) and 10(b),

 

respectively, plot the effect of $v/v'$ (Rocks 1, 4, 5) with $\alpha = -1$, $\beta = -1, \alpha = \beta = 0$, $\alpha = 1$, and $\beta = 1$ on the vertical stress. According to these figures, the induced stress is slightly influenced by $v/v'$. Figures 6–10 show that the vertical stress increases with the non-dimensional factor, $n$, for all rocks, implying that the stress calculated from plane strain exceeds the three-dimensional solution. The figures also indicate that the stress induced by the considered loading types strongly depends on the dimensions of the loaded area, and the type and degree of rock anisotropy.

Figures 11(a)–11(g) clarify the effect of the loading ($\alpha = -1$, $\beta = -1$, $\alpha = \beta = 0$, $\alpha = 1$, $\beta = 1$) on the non-dimensional vertical stress ($\sigma_{zz}^{\text{linear}}/P_z^{\text{linear}}$ or $\sigma_{zz}^{\text{par}}/P_z^{\text{par}}$) for Rocks 1–7, respectively, with $n = 1.0$. Figures 11(a)–11(e) show that the order induced stress follows $\alpha = 1 > \beta = 1 > \alpha = \beta = 0 > \beta = -1 > \alpha = -1$. The magnitude of the calculated stress can be reasonably judged from the geometry of loading in Figures 1–4. However, the trend in the induced stress in Figures 11(f) and 11(g) (for Rocks 6 and 7) differs a little from that in Figures 11(a)–11(e), within the smaller loaded region ($m \leqslant 2$). Figures 11(a)–11(e) show the effect of the loading type on the stress is explicit. The average induced vertical stress by $\alpha = 1$ and $\beta = 1$ is approximately double that induced by $\alpha = \beta = 0$ for all rocks; however, the average stress by $\alpha = -1$ and $\beta = -1$ is disproportional to that by $\alpha = \beta = 0$.

The example was presented to elucidate the solutions and clarify how the dimensions of the loaded area, the type and degree of rock anisotropy, and the type of loading affect the non-dimensional vertical stress. The analysis results indicate that the induced stress in isotopic/transversely isotropic rocks under various types of loading is easily calculated. Hence, the anisotropic deformability must be considered when estimating the stresses in a transversely isotropic half-space subjected to linearly varying/uniform/parabolic rectangular loads.

## 4. CONCLUSIONS

Integrating the elementary functions of a point load yields the elastic solutions for stresses in a transversely isotropic half-space subjected to three-dimensional, buried, linearly varying, uniform and parabolic rectangular loads. The solutions are limited to planes of transverse isotropy that are parallel to the horizontal surface of the half-space. The loading types include an upwardly linearly varying load, a downwardly linearly varying load, a uniform load, a concave parabolic load and a convex parabolic load, all acting on a rectangular area. The proposed closed-form solutions for stresses are affected by the buried depth ($h$), the dimensions of the loaded area ($L, W$), the type and degree of rock anisotropy ($E/E', v/v', G/G'$), and the type of loading ( $\alpha > 0$, $\alpha = \beta = 0$, $\alpha < 0$, $\beta > 0$, $\beta < 0$) in transversely isotropic half-spaces.

A parametric study of an illustrative example has yielded the following conclusions:

1. The ratios $E/E'$ ($\upsilon/\upsilon' = G/G' = 1$) and $G/G'$ ($E/E' = v/v' = 1$) strongly influence the non-dimensional vertical stress in transversely isotropic rocks subjected to a downwardly linearly varying, and a convex parabolic rectangular load. However, $\upsilon/\upsilon'$ ($E/E' = G/G' = 1$) has little effect on this stress.
2. In a very small loaded area of $m$ and $n$, a little stress may be transferred by tension in the medium.

 

3. The stress induced in transversely isotropic rocks by a uniform, an upwardly linearly varying and a concave parabolic rectangular load decreases as $E/E'$ increases, and increases as $G/G'$ increases, but is only slightly influenced by $\upsilon/\upsilon'$.
4. The plane strain solution overestimates the induced stress, as compared to the presented three-dimensional solution.
5. The induced stress heavily relies on the dimensions of the loaded area, the type and degree of material anisotropy, and the type of loading types.
6. The formulated stresses correlate well with those in the isotropic medium under plane strain.

The calculation of induced stresses by various types of loading, distributed over a rectangular area in an isotropic/transversely isotropic half-space is fast and correct, and the presentation of the derived solutions is clear and concise. These solutions can more realistically simulate actual loading circumstances in many engineering practices. Furthermore, the presented solutions also offer an alternative to the numerical or graphical methods, and provide reasonable results for practical purposes.

Similarly, the elastic solutions for displacements in a transversely isotropic half-space subjected to the types of loading considered here can also be derived. The solutions will be presented in forthcoming papers [19].

## APPENDIX A

The point load solutions for stresses in a transversely isotropic half-space in Cartesian forms can be expressed as follows [6]:

$$\begin{aligned}
\sigma_{xx}^{p} = \frac{P_x}{4\pi}\Bigg[ & (A_{11} - u_1 m_1 A_{13})\left(\frac{k}{m_1}\, p_{s11} - T_1\, p_{s1a} + T_2\, p_{s1b}\right) \\
& - (A_{11} - u_2 m_2 A_{13})\left(\frac{k}{m_2}\, p_{s12} - T_3\, p_{s1c} + T_4\, p_{s1d}\right) \\
& - 2A_{66}\left(\frac{k}{m_1}\, p_{s71} - \frac{k}{m_2}\, p_{s72} - T_1\, p_{s7a} + T_2\, p_{s7b} + T_3\, p_{s7c} - T_4\, p_{s7d}\right) + 2u_3(p_{s73} + p_{s7e})\Bigg] \\
& + \frac{P_y}{4\pi}\Bigg[(A_{11} - u_1 m_1 A_{13} - 2A_{66})\left(\frac{k}{m_1}\, p_{s21} - T_1\, p_{s2a} + T_2\, p_{s2b}\right) \\
& - (A_{11} - u_2 m_2 A_{13} - 2A_{66})\left(\frac{k}{m_2}\, p_{s22} - T_3\, p_{s2c} + T_4\, p_{s2d}\right) \\
& + 2A_{66}\left(\frac{k}{m_1}\, p_{s81} - \frac{k}{m_2}\, p_{s82} - T_1\, p_{s8a} + T_2\, p_{s8b} + T_3\, p_{s8c} - T_4\, p_{s8d}\right) - 2u_3(p_{s83} + p_{s8e})\Bigg] \\
& + \frac{P_z}{4\pi}\{(A_{11} - u_1 m_1 A_{13} - 2A_{66})(k\, p_{s31} + T_1 m_1\, p_{s3a} - T_2 m_2\, p_{s3b}) \\
& - (A_{11} - u_2 m_2 A_{13} - 2A_{66})(k\, p_{s32} + T_3 m_1\, p_{s3c} - T_4 m_2\, p_{s3d}) \\
& + 2A_{66}[k(p_{s51} - p_{s52}) + m_1(T_1\, p_{s5a} - T_3\, p_{s5c}) - m_2(T_2\, p_{s5b} - T_4\, p_{s5d})]\}
\end{aligned} \tag{A1}$$

 

$$\sigma_{yy}^{p}=\frac{P_x}{4\pi}\Bigg[(A_{11}-u_1m_1A_{13}-2A_{66})\left(\frac{k}{m_1}\,p_{s11}-T_1\,p_{s1a}+T_2\,p_{s1b}\right)$$
$$-\,(A_{11}-u_2m_2A_{13}-2A_{66})\left(\frac{k}{m_2}\,p_{s12}-T_3\,p_{s1c}+T_4\,p_{s1d}\right)$$
$$+2A_{66}\left(\frac{k}{m_1}\,p_{s71}-\frac{k}{m_2}\,p_{s72}-T_1\,p_{s7a}+T_2\,p_{s7b}+T_3\,p_{s7c}-T_4\,p_{s7d}\right)-2u_3(p_{s73}+p_{s7e})\Bigg]$$
$$+\,\frac{P_y}{4\pi}\Bigg[(A_{11}-u_1m_1A_{13})\left(\frac{k}{m_1}\,p_{s21}-T_1\,p_{s2a}+T_2\,p_{s2b}\right)$$
$$-\,(A_{11}-u_2m_2A_{13})\left(\frac{k}{m_2}\,p_{s22}-T_3\,p_{s2c}+T_4\,p_{s2d}\right)$$
$$-2A_{66}\left(\frac{k}{m_1}\,p_{s81}-\frac{k}{m_2}\,p_{s82}-T_1\,p_{s8a}+T_2\,p_{s8b}+T_3\,p_{s8c}-T_4\,p_{s8d}\right)+2u_3(p_{s83}+p_{s8e})\Bigg] \tag{A2}$$
$$+\,\frac{P_z}{4\pi}\{(A_{11}-u_1m_1A_{13}-2A_{66})(kp_{s31}+T_1m_1\,p_{s3a}-T_2m_2\,p_{s3b})$$
$$-\,(A_{11}-u_2m_2A_{13}-2A_{66})(kp_{s32}+T_3m_1\,p_{s3c}-T_4m_2\,p_{s3d})$$
$$+\,2A_{66}[k(p_{s61}-p_{s62})+m_1(T_1\,p_{s6a}-T_3\,p_{s6c})-m_2(T_2\,p_{s6b}-T_4\,p_{s6d})]\}$$

$$\sigma_{zz}^{p}=\frac{P_x}{4\pi}\left[(A_{13}-u_1m_1A_{33})\left(\frac{k}{m_1}\,p_{s11}-T_1\,p_{s1a}+T_2\,p_{s1b}\right)\right.$$
$$\left.-\,(A_{13}-u_2m_2A_{33})\left(\frac{k}{m_2}\,p_{s12}-T_3\,p_{s1c}+T_4\,p_{s1d}\right)\right]$$
$$+\,\frac{P_y}{4\pi}\left[(A_{13}-u_1m_1A_{33})\left(\frac{k}{m_1}\,p_{s21}-T_1\,p_{s2a}+T_2\,p_{s2b}\right)\right.$$
$$\left.-\,(A_{13}-u_2m_2A_{33})\left(\frac{k}{m_2}\,p_{s22}-T_3\,p_{s2c}+T_4\,p_{s2d}\right)\right]$$
$$+\,\frac{P_z}{4\pi}[(A_{13}-u_1m_1A_{33})(kp_{s31}+T_1m_1\,p_{s3a}-T_2m_2\,p_{s3b})$$
$$-\,(A_{13}-u_2m_2A_{33})(kp_{s32}+T_3m_1\,p_{s3c}-T_4m_2\,p_{s3d})] \tag{A3}$$

$$\tau_{xy}^{p}=\frac{P_x}{4\pi}\left[2A_{66}\left(\frac{k}{m_1}\,p_{s81}-\frac{k}{m_2}\,p_{s82}-T_1\,p_{s8a}+T_2\,p_{s8b}+T_3\,p_{s8c}-T_4\,p_{s8d}\right)\right.$$
$$\left.-\,u_3(2\,p_{s83}+2\,p_{s8e}-p_{s23}-p_{s2e})\right]$$
$$+\,\frac{P_y}{4\pi}\left[2A_{66}\left(\frac{k}{m_1}\,p_{s71}-\frac{k}{m_2}\,p_{s72}-T_1\,p_{s7a}+T_2\,p_{s7b}+T_3\,p_{s7c}-T_4\,p_{s7d}\right)\right.$$
$$\left.-\,u_3(2\,p_{s73}+2\,p_{s7e}-p_{s13}-p_{s1e})\right]$$
$$-\,\frac{P_z}{2\pi}A_{66}[k(p_{s41}-p_{s42})+m_1(T_1\,p_{s4a}-T_3\,p_{s4c})-m_2(T_2\,p_{s4b}-T_4\,p_{s4d})] \tag{A4}$$

 

$$\tau_{yz}^{p} = -\frac{P_x}{4\pi}\left[(u_1+m_1)A_{44}\left(\frac{k}{m_1}\,p_{s41} - T_1\,p_{s4a} + T_2\,p_{s4b}\right)\right.$$
$$\left. -(u_2+m_2)A_{44}\left(\frac{k}{m_2}\,p_{s42} - T_3\,p_{s4c} + T_4\,p_{s4d}\right) - (p_{s43}+p_{s4e})\right]$$
$$+\frac{P_y}{4\pi}\left[(u_1+m_1)A_{44}\left(\frac{k}{m_1}\,p_{s61} - T_1\,p_{s6a} + T_2\,p_{s6b}\right)\right.$$
$$\left. -(u_2+m_2)A_{44}\left(\frac{k}{m_2}\,p_{s62} - T_3\,p_{s6c} + T_4\,p_{s6d}\right) + (p_{s53}+p_{s5e})\right]$$
$$-\frac{P_z}{4\pi}A_{44}[(u_1+m_1)(k\,p_{s21} + T_1 m_1\,p_{s2a} - T_2 m_2\,p_{s2b})$$
$$-(u_2+m_2)(k\,p_{s22} + T_3 m_1\,p_{s2c} - T_4 m_2\,p_{s2d})] \tag{A5}$$

$$\tau_{xz}^{p} = \frac{P_x}{4\pi}\left[(u_1+m_1)A_{44}\left(\frac{k}{m_1}\,p_{s51} - T_1\,p_{s5a} + T_2\,p_{s5b}\right)\right.$$
$$\left. -(u_2+m_2)A_{44}\left(\frac{k}{m_2}\,p_{s52} - T_3\,p_{s5c} + T_4\,p_{s5d}\right) + (p_{s63}+p_{s6e})\right]$$
$$-\frac{P_y}{4\pi}\left[(u_1+m_1)A_{44}\left(\frac{k}{m_1}\,p_{s41} - T_1\,p_{s4a} + T_2\,p_{s4b}\right)\right.$$
$$\left. -(u_2+m_2)A_{44}\left(\frac{k}{m_2}\,p_{s42} - T_3\,p_{s4c} + T_4\,p_{s4d}\right) - (p_{s43}+p_{s4e})\right]$$
$$-\frac{P_z}{4\pi}A_{44}[(u_1+m_1)(k\,p_{s11} + T_1 m_1\,p_{s1a} - T_2 m_2\,p_{s1b})$$
$$-(u_2+m_2)(k\,p_{s12} + T_3 m_1\,p_{s1c} - T_4 m_2\,p_{s1d})] \tag{A6}$$

where

- $A_{ij}$ $(i,j = 1\text{–}6)$ are the elastic moduli or elasticity constants of the medium, and can be expressed in terms of five independent elastic constants for a transversely isotropic half-space as

$$A_{11} = \frac{E(1-(E/E')\upsilon'^2)}{(1+\upsilon)(1-\upsilon-(2E/E')\upsilon'^2)}, \quad A_{13} = \frac{E\upsilon'}{1-\upsilon-(2E/E')\upsilon'^2},$$
$$A_{33} = \frac{E'(1-\upsilon)}{1-\upsilon-(2E/E')\upsilon'^2}, \quad A_{44} = G', \quad A_{66} = \frac{E}{2(1+\upsilon)} \tag{A7}$$

  where $E$ and $E'$ are Young's moduli in the plane of transverse isotropy and in a direction normal to it, respectively; $\upsilon$ and $\upsilon'$ are Poisson's ratios characterizing the lateral strain response in the plane of transverse isotropy to a stress acting parallel and normal to it, respectively; $G'$ is the shear modulus in planes normal to the plane of transverse isotropy.
- $u_3 = \sqrt{A_{66}/A_{44}}$, $u_1$ and $u_2$ are the roots of the following characteristic equation:

$$u^4 - su^2 + q = 0 \tag{A8}$$

 

whereas

$$s = \frac{A_{11}A_{33} - A_{13}(A_{13} + 2A_{44})}{A_{33}A_{44}}, \quad q = \frac{A_{11}}{A_{33}}.$$

Since the strain energy is assumed to be positive definite in the medium, the values of elastic constants are restricted. Hence, there are three categories of the characteristic roots, $u_1$ and $u_2$ as follows:

*Case* 1: $u_{1,2} = \pm\sqrt{\{\frac{1}{2}[s \pm \sqrt{(s^2 - 4q)}]\}}$ are two real distinct roots when $s^2 - 4q > 0$;

*Case* 2: $u_{1,2} = \pm\sqrt{s/2}, \pm\sqrt{s/2}$ are double equal real roots when $s^2 - 4q = 0$;

*Case* 3: $u_1 = \frac{1}{2}\sqrt{(s + 2\sqrt{q})} - i\frac{1}{2}\sqrt{(-s + 2\sqrt{q})} = \gamma - i\delta$, $u_2 = \gamma + i\delta$ are two complex conjugate roots (where $\gamma$ cannot be equal to zero) when $s^2 - 4q < 0$.

- $m_j = \dfrac{(A_{13} + A_{44})u_j}{A_{33}u_j^2 - A_{44}} = \dfrac{A_{11} - A_{44}u_j^2}{(A_{13} + A_{44})u_j}\ (j = 1, 2)$, $k = \dfrac{(A_{13} + A_{44})}{A_{33}A_{44}(u_1^2 - u_2^2)}$, $T_1 = \dfrac{k}{m_1}\dfrac{u_1 + u_2}{u_2 - u_1}$

$$T_2 = \frac{k}{m_2}\frac{2u_1(u_2 + m_2)}{(u_2 - u_1)(u_1 + m_1)}, \quad T_3 = \frac{k}{m_1}\frac{2u_2(u_1 + m_1)}{(u_2 - u_1)(u_2 + m_2)}, \quad T_4 = \frac{k}{m_2}\frac{u_1 + u_2}{u_2 - u_1};$$

$$p_{s1i} = \frac{x}{R_i^3}\ \ p_{s2i} = \frac{y}{R_i^3}, \quad p_{s3i} = \frac{z_i}{R_i^3}, \quad p_{s4i} = \frac{xy(2R_i + z_i)}{R_i^3(R_i + z_i)^2}, \quad p_{s5i} = \frac{1}{R_i(R_i + z_i)} - \frac{x^2(2R_i + z_i)}{R_i^3(R_i + z_i)^2}$$

$$p_{s6i} = \frac{1}{R_i(R_i + z_i)} - \frac{y^2(2R_i + z_i)}{R_i^3(R_i + z_i)^2}, \quad p_{s7i} = \frac{x}{R_i^3} - \frac{3x}{R_i(R_i + z_i)^2} + \frac{x^3(3R_i + z_i)}{R_i^3(R_i + z_i)^3}$$

$$p_{s8i} = \frac{y}{R_i^3} - \frac{3y}{R_i(R_i + z_i)^2} + \frac{y^3(3R_i + z_i)}{R_i^3(R_i + z_i)^3}$$

- $R_i = \sqrt{x^2 + y^2 + z_i^2}$ $(i = 1, 2, 3, a, b, c, d, e)$, $z_1 = u_1(z - h)$, $z_2 = u_2(z - h)$, $z_3 = u_3(z - h)$, $z_a = u_1(z + h)$, $z_b = u_1 z + u_2 h$, $z_c = u_1 h + u_2 z$, $z_d = u_2(z + h)$, $z_e = u_3(z + h)$. The load is applied at the surface when the buried depth $h = 0$.

## APPENDIX B: NOMENCLATURE

| | |
|---|---|
| $A_{ij}(i, j = 1-6)$ | elastic moduli or elastic constants in Equation (A7) |
| $d\eta$, $d\zeta$ | infinitesimal element along $Y$- or $X$-axis, respectively |
| $E$, $E'$, $\upsilon$, $\upsilon'$, $G'$ | engineering elastic constants of transversely isotropic materials |
| $h$ | the buried depth, as seen in Figures 1–4 |
| $i$ | complex number $(= \sqrt{-1})$ |
| $k, m_1, m_2, T_1, T_2, T_3, T_4$ | coefficients in Equations (A1)–(A6) |
| $L, W$ | length along $X$-axis and width along $Y$-axis, respectively |
| $N_{s1i}^{\langle 1\rangle} - N_{s1i}^{\langle 9\rangle}, \ldots, N_{s8i}^{\langle 1\rangle}$–$N_{s8i}^{\langle 9\rangle}$ | integral functions for stresses induced by linearly varying, uniform, and parabolic rectangular loads |
| $p_{s1i} \sim p_{s8i}$ | elementary functions for stresses induced by a point load |
| $P_j$ $(j = x, y, z)$ | a point load (force) |

 

| | |
|---|---|
| $P_j^{\text{linear}}$ $(j = x, y, z)$ | linearly varying rectangular loads (forces per unit of area) |
| $P_j^{\text{par}}$ $(j = x, y, z)$ | parabolic rectangular loads (forces per unit of area) |
| $q, s$ | coefficients in Equation (A8) |
| $u_1, u_2, u_3$ | roots of the characteristic equation (Equation (A8)) |
| $X, Y, Z$ | Cartesian co-ordinate system |

*Greek letters*

| | |
|---|---|
| $\alpha$, $\beta$ | the constant controlling the linearly varying and parabolic loads, respectively |
| $\gamma, \delta$ | real and imaginary part of the complex roots, respectively |
| $\sigma$ | stress components |
| $\sigma_{xx}^{\text{linear}}, \sigma_{yy}^{\text{linear}}, \sigma_{zz}^{\text{linear}}$ | normal stresses induced by linearly varying rectangular loads |
| $\sigma_{xx}^{p}, \sigma_{yy}^{p}, \sigma_{zz}^{p}$ | normal stresses induced by a point load |
| $\sigma_{xx}^{\text{par}}, \sigma_{yy}^{\text{par}}, \sigma_{zz}^{\text{par}}$ | normal stresses induced by parabolic rectangular loads |
| $\tau_{xy}^{\text{linear}}, \tau_{yz}^{\text{linear}}, \tau_{xz}^{\text{linear}}$ | shear stresses induced by linearly varying rectangular loads |
| $\tau_{xy}^{p}, \tau_{yz}^{p}, \tau_{xz}^{p}$ | shear stresses induced by a point load |
| $\tau_{xy}^{\text{par}}, \tau_{yz}^{\text{par}}, \tau_{xz}^{\text{par}}$ | shear stresses induced by parabolic rectangular loads |

*Superscripts*

| | |
|---|---|
| linear | stresses induced by linearly varying rectangular loads |
| $p$ | stresses induced by a point load |
| par | stresses induced by parabolic rectangular loads |
| T | transpose matrix |

ACKNOWLEDGEMENT

The authors would like to thank the National Science Council of the Republic of China for financially supporting this research under Contract No. NSC 91-2211-E-253-002.

REFERENCES

1. Wang CD, Liao JJ. Stress influence charts for transversely isotropic rocks. *International Journal of Rock Mechanics and Mining Sciences* 1998; **35**:771–785.
2. Wang CD, Liao JJ. Computing displacements in transversely isotropic rocks using influence charts. *Rock Mechanics and Rock Engineering* 1999; **32**:51–70.
3. Lekhnitskii SG. *Theory of Elasticity of an Anisotropic Elastic Body*. Holden-Day Press: San Francisco, 1963.
4. Pan YC, Chou TW. Green's function solutions for semi-infinite transversely isotropic materials. *International Journal of Engineering Science* 1979; **17**:545–551.
5. Liao JJ, Wang CD. Elastic solutions for a transversely isotropic half-space subjected to a point load. *International Journal for Numerical and Analytical Methods in Geomechanics* 1998; **22**:425–447.
6. Wang CD, Liao JJ. Elastic solutions for a transversely isotropic half-space subjected to buried asymmetric-loads. *International Journal for Numerical and Analytical Methods in Geomechanics* 1999; **23**:115–139.
7. Wang CD, Liao JJ. Elastic solutions for a transversely isotropic half-space subjected to arbitrarily-shaped loads using triangulating technique. *International Journal of Geomechanics* 2001; **1**:193–224.
8. Lin W, Kuo CH, Keer LM. Analysis of a transversely isotropic half space under normal and tangential loadings. *Journal of Tribology ASME* 1991; **113**:335–338.
9. Hooper JA. Parabolic adhesive loading of a flexible raft foundation. *Geotechnique* 1976; **26**:511–525.
10. Bauer GE, Shields DH, Scott JD, Nwabuokei SO. Normal and shear measurements on a strip footing. *Canadian Geotechnical Journal* 1979; **16**:177–189.

 

11. Teferra A, Schultze E. *Formulae, Charts and Tables in the Area of Soil Mechanics and Foundation Engineering, Stresses in Soils*. A. A. Balkema Publishers: Brookfield, 1988.
12. Gazetas G. Stresses and displacements in cross-anisotropic soils. *Journal of Geotechnical Engineering Division ASCE* 1982; **108**:532–553.
13. Gazetas G. Axisymmetric parabolic loading of anisotropic halfspace. *Journal of Geotechnical Engineering Division ASCE* 1982; **108**:654–660.
14. Davis RO, Selvadurai APS. *Elasticity and Geomechanics*. Cambridge University Press: New York, 1996.
15. Gerrard CM. Background to mathematical modeling in geomechanics: the roles of fabric and stress history. *Proceedings of International Symposium on Numerical Methods*, Karlsruhe, 1975; 33–120.
16. Amadei B, Savage WZ, Swolfs HS. Gravitational stresses in anisotropic rock masses. *International Journal of Rock Mechanics and Mining Sciences & Geomechanics Abstract* 1987; **24**:5–14.
17. Feda J. *Stress in Subsoil and Methods of Final Settlement Calculation*. Elsevier Scientific Publishing Company: Amsterdam, 1978.
18. Giroud JP. *Tables Pour Le Calcul Des Fondations*. Tome.2. Tassement: Dunod, 1973.
19. Wang CD, Liao JJ. Elastic solutions of displacements for a transversely isotropic half-space subjected to three-dimensional buried parabolic rectangular loads. *International Journal of Solids and Structures* 2002; in press.

 